Stem Cell Reports
Article

ISSCR

OPEN ACCESS

Neural Stem Cell Differentiation Is Dictated by Distinct Actions of Nuclear Receptor Corepressors and Histone Deacetylases

Gonçalo Castelo-Branco,[1,2,*] Tobias Lilja,[1] Karolina Wallenborg,[1] Ana M. Falcão,[1,2] Sueli C. Marques,[2] Aileen Gracias,[1] Derek Solum,[3] Ricardo Paap,[1] Julian Walfridsson,[1] Ana I. Teixeira,[1] Michael G. Rosenfeld,[3] Kristen Jepsen,[3] and Ola Hermanson[1,*]

[1]Linnaeus Center in Developmental Biology for Regenerative Medicine (DBRM), Department of Neuroscience, Karolinska Institutet, 17177 Stockholm, Sweden
[2]Laboratory of Molecular Neurobiology, Department of Medical Biochemistry and Biophysics, Karolinska Institutet, 17177 Stockholm, Sweden
[3]Howard Hughes Medical Institute, Department of Medicine, University of California, San Diego (UCSD), 9500 Gilman Drive, La Jolla, CA 92093-0648, USA
*Correspondence: goncalo.castelo-branco@ki.se (G.C.-B.), ola.hermanson@ki.se (O.H.)
http://dx.doi.org/10.1016/j.stemcr.2014.07.008

SUMMARY

Signaling factors including retinoic acid (RA) and thyroid hormone (T3) promote neuronal, oligodendrocyte, and astrocyte differentiation of cortical neural stem cells (NSCs). However, the functional specificity of transcriptional repressor checkpoints controlling these differentiation programs remains unclear. Here, we show by genome-wide analysis that histone deacetylase (HDAC)2 and HDAC3 show overlapping and distinct promoter occupancy at neuronal and oligodendrocyte-related genes in NSCs. The absence of HDAC3, but not HDAC2, initiated a neuronal differentiation pathway in NSCs. The ablation of the corepressor NCOR or HDAC2, in conjunction with T3 treatment, resulted in increased expression of oligodendrocyte genes, revealing a direct HDAC2-mediated repression of *Sox8* and *Sox10* expression. Interestingly, *Sox10* was required also for maintaining the more differentiated state by repression of stem cell programming factors such as *Sox2* and *Sox9*. Distinct and nonredundant actions of NCORs and HDACs are thus critical for control of lineage progression and differentiation programs in neural progenitors.

INTRODUCTION

Histone-deacetylase-associated (HDAC-associated) DNA-binding transcription factors, including REST (also known as neuron-restrictive silencer factor [NRSF]) and coregulators such as the nuclear receptor corepressor (NCOR/Ncor1) and silencing mediator of retinoic acid and thyroid hormone receptors (SMRT/Ncor2), have been shown to be essential regulators of neural proliferation and differentiation during brain development, as they actively repress lineage-characteristic gene expression and are required for self-renewal or progression of cell fate specification (Andreu-Agulló et al., 2009; Ballas et al., 2005; Hermanson et al., 2002b; Jepsen et al., 2007; Johnson et al., 2008; Lilja et al., 2013a; Miller and Gauthier, 2007; Wang et al., 2010). Mammalian HDACs can be divided into several classes, with the class I HDACs most strongly associated with NCOR and SMRT (Yang and Seto, 2008). NCOR and/or SMRT-HDAC complexes regulate histone modifications occurring at single lysines of histone tails that seem to display progenitor-specific signatures (Spivakov and Fisher, 2007). These modified lysines in turn function as molecular beacons recruiting specific complexes for regulation of gene expression (Perissi et al., 2010; Ruthenburg et al., 2007). Studies using inhibitors of HDACs, including valproic acid (VPA), have established that such compounds can affect the differentiation of embryonic and adult neural progenitors both negatively and positively and also exert toxic effects on neuroectodermal cells (Hsieh et al., 2004; Laeng et al., 2004; Marin-Husstege et al., 2002; Salminen et al., 1998). Genetic models of HDAC1 and HDAC2 ablation also support roles for class I HDACs in regulating forebrain neural progenitor characteristics, although the roles for individual HDACs remain unclear (Montgomery et al., 2009; Ye et al., 2009).

Despite the neurodevelopmental phenotypes and neural progenitor aberrations of mice harboring genetic deletions of *Ncor* versus *Smrt* being distinct (Hermanson et al., 2002b; Jepsen et al., 2000, 2007), functional and nonredundant specificity regarding the associated HDACs is not well understood (Perissi et al., 2010). HDAC activity has been shown to both be required and repressive for neurogenesis (Hsieh et al., 2004; Montgomery et al., 2009). Likewise, HDAC activity can be required for oligodendrocyte differentiation and proper myelination (Ye et al., 2009). However, HDAC inhibitors such as VPA have also been shown to have positive effects on oligodendrocyte generation and function (Liu et al., 2012), and the alleviation of transcription factors associated with HDAC complexes, such as REST (NRSF), results in increased expression of oligodendrocyte genes (Covey et al., 2012). Only a few studies have addressed the roles for individual HDACs and histone acetyl transferases (HATs) in oligodendrocyte differentiation of embryonic forebrain progenitors using genetic mouse models (Wang et al., 2010; Ye et al., 2009). The deletion of *Hdac1* or *Hdac2* individually in NSCs only had

limited effects, while simultaneous deletion of the two factors resulted in a loss of markers of oligodendrocyte differentiation in cortical progenitors (Ye et al., 2009). Paradoxically, genetic and RNA knockdown of the HAT *Cbp* (also known as *Crebbp*) in the embryonic forebrain also resulted in decreased expression of oligodendrocyte markers in cortical NSCs, and *Cbp* haploinsufficiency leads to aberrant development of the corpus callosum (Wang et al., 2010).

To elucidate the roles for these factors in differentiation of cortical progenitors, we undertook an investigation of the functional roles for class I HDACs and nuclear receptor corepressors in the enforcement of NSC repression checkpoints that are subsequently released during differentiation to neurons and glia. By analysis of NSCs derived from rodents with gene deletions and/or specific RNA knockdown in wild-type primary-derived NSCs, we have revealed a series of distinct functional roles for the class I HDACs, HDAC2, and HDAC3, alone and in concert with NCOR or SMRT in the regulation of NSC differentiation into neurons and oligodendrocytes.

RESULTS

HDAC2 and HDAC3 Show Both Unique and Overlapping Binding to Promoter Regions of Genes Associated with Neuronal and Oligodendrocyte Differentiation

To investigate specific roles for HDAC2 and HDAC3, we performed chromatin immunoprecipitation sequencing (ChIP-seq) (Gene Expression Omnibus [GEO] accession GSE57232; see Füllgrabe et al., 2013; Heldring et al., 2014) and subsequent single-gene ChIP analysis (see Lilja et al., 2013b) in neural stem cells (NSCs) derived from embryonic cortices of rats at embryonic day 15 (E15), which produce HDAC2 and HDAC3, but not HDAC1 (Figure 1C). HDAC2 and HDAC3 were determined to be present in the vicinity of a number of genes associated with transcriptional regulation of differentiation (Figure 1A). Several of the regions identified by ChIP-seq were confirmed by subsequent single-gene ChIP-quantitative PCR (ChIP-qPCR) experiments that demonstrated that HDAC2 and HDAC3 could bind both in an overlapping and distinct fashion near genes associated with development and differentiation, including *Cebpb* (C/EBPβ), *Hoxd4*, *Ovol2*, and *Zfp7* (Figure 1A; data not shown). A more detailed analysis revealed differences in enrichment at certain genes critically involved in NSC differentiation. Whereas a significant enrichment of HDAC3 was found on the promoters of both *Pax6* and *Sox8*, genes encoding transcription factors associated with neuronal and oligodendrocyte differentiation of NSCs, increased enrichment of HDAC2 was only found on the *Sox8* promoter (Figure 1B). This observation was of particular interest due to a previous report demonstrating that class I HDACs, including HDAC2, are essential for proper progression of embryonic oligodendrocyte development (Ye et al., 2009).

Similar to SMRT, HDAC3 Represses Neuronal Genes in Embryonic NSCs

While previous analyses of the functional roles for HDAC1 and HDAC2 by genetic mouse models have confirmed redundant roles for the two factors in embryonic development of the nervous system, our ChIP analysis suggested that there could be functional differences between HDAC2 and HDAC3 in embryonic NSCs. To examine the individual role(s) of these class I HDACs in NSCs, specific small interference RNA (siRNA) pools were used to rapidly and conditionally knockdown *Hdac2* and *Hdac3* mRNA in the cortically derived NSCs (see Figures S1A and S1B available online for efficiency of the siRNAs). NSCs transfected with siHDAC3 or a combination of siHDAC2 and siHDAC3 showed global hyperacetylation of H3K9 (Figure 1E) and a significant increase in TuJ1-positive cells (Figure 1D), as well as an increased H3K9 acetylation on the well-established HDAC target *Bdnf* IV promoter as compared to control siRNA (Figure 1F). In contrast, transfection of siHDAC2 had no significant effect on these parameters (Figures 1D–1F). Analysis of gene expression by quantitative RT-PCR (qRT-PCR) showed that siHDAC2 treatment had no significant effect on *Bdnf* mRNA levels in NSCs, whereas siHDAC3 delivery alone was sufficient to induce a significant increase in *Bdnf* gene expression (Figure 1G). As the gene encoding TUBB3, the protein detected by the antibody TuJ1, is a direct target for the HDAC-associated repressor REST, it is possible that the increase in TuJ1-positive cells could be due to a direct regulation and increased acetylation at the *Tubb3* gene. We however also noted an increase in expression of the proneuronal gene *Neurog2* 6–24 hr after siHDAC3 delivery (data not shown), pointing to multiple putative mechanisms that could underlie increased neuronal differentiation and survival after siHDAC3 delivery. Together, these results demonstrate that HDAC3, but not HDAC2, is a nonredundant repressor of H3K9 acetylation, *Bdnf* gene expression, and neuronal differentiation in cortical NSCs.

To shed further light on the mechanisms underlying the functional specificity of HDAC2 and HDAC3, we turned to the closely associated nuclear receptors NCOR and SMRT. These HDAC-associated corepressors have in spite of their sequence homology previously been shown to play distinct functional roles in NSCs as spontaneous neuronal and astrocytic differentiation has been noted only in NSCs derived from *Smrt*-deficient mice, while only astrocytic and no neuronal differentiation has been reported in

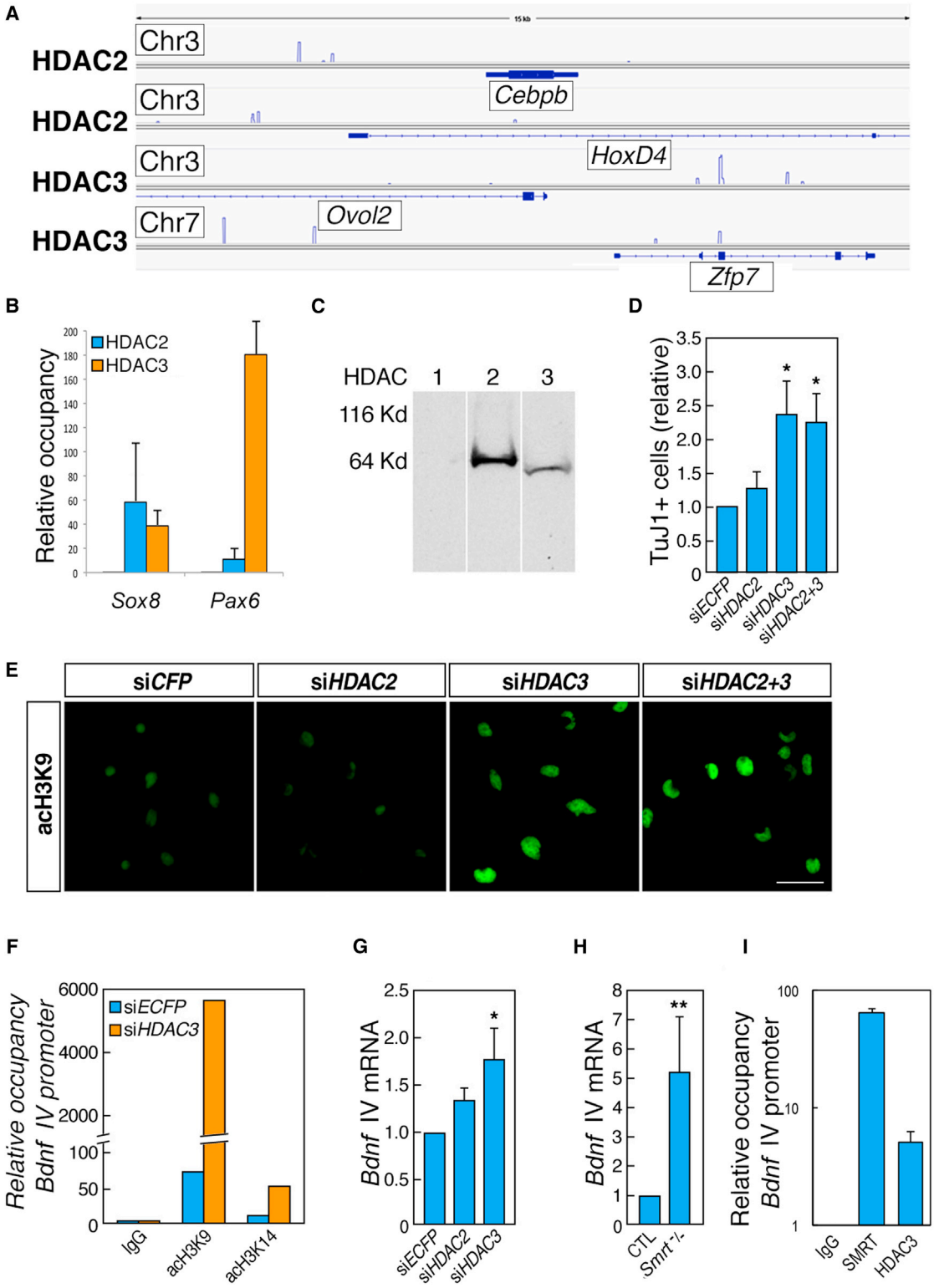

Figure 1. Single-Gene and Genome-wide ChIP Reveal Overlapping and Nonoverlapping Occupancies of HDAC2 and HDAC3 and HDAC3, but Not HDAC2, Knockdown Results in Increased Neuronal Differentiation of NSCs

(A) Genome browser images of normalized densities of HDAC2 and HDAC3 on regions of chromosomes 3 and 7 in the vicinity of genes encoding *Cebpb*, *Ovol2*, *Hoxd4*, and *Zfp7* in cortically derived NSCs.

(legend continued on next page)

NSCs from *Ncor*-deficient or double-heterozygote mice (Hermanson et al., 2002b; Jepsen et al., 2007). ChIP analysis revealed that both SMRT and HDAC3 were enriched at the *Bdnf* IV promoter, and qRT-PCR investigation of *Bdnf* gene expression levels in $Smrt^{-/-}$ NSCs revealed a significant (>4-fold) increase compared to wild-type cells (Figures 1H and 1I). In contrast, *Bdnf* mRNA levels in $Ncor^{-/-}$ NSCs, which do not differentiate down the neuronal pathway, remained unchanged (data not shown; see further below). This result suggests that HDAC3, rather than HDAC2, is involved in at least a subset of the critical SMRT-mediated repressive events in NSCs.

Absence of the T3-Associated Corepressor NCOR Promotes Oligodendrocyte-Associated Gene Expression

NSCs derived from mice gene-deleted for either *Ncor* or *Smrt*, or from double-heterozygote animals, spontaneously differentiate into astrocytes, suggesting that regulation of this pathway depends on proper gene dosage of both *Ncor* and *Smrt* (Hermanson et al., 2002b; Jepsen et al., 2007). Interestingly, a substantial subset of the $Ncor^{-/-}$ NSCs display neither the astrocytic marker GFAP nor the stem cell marker nestin or neuronal marker TuJ1 (Hermanson et al., 2002b), suggesting the possibility that NCOR represses additional NSC fates. Indeed, gene expression profiling analysis by microarrays of $Ncor^{-/-}$ NSCs after 4 days in vitro (DIV) revealed a dramatic upregulation of several oligodendrocyte (OL)-associated genes, including myelin-basic protein (*Mbp*), myelin proteolipid protein (*Plp*), *beta tubulin 4*, and *Nkx2.2*, as well as early pan-glial markers such as *S100β*, whereas no significant upregulation of neuronal genes was detected (Figure 2B; Hermanson et al., 2002b). In contrast, gene expression profiling of $Smrt^{-/-}$ NSCs or NSCs treated with the HDAC inhibitor valproic acid (VPA) failed to detect any upregulation of OL-associated genes (Figure S2A; Figure S4 in Jepsen et al., 2007). Detailed analysis revealed that approximately 18% of $Ncor^{-/-}$ NSCs stained positive for the archetypical OL marker MBP and presented morphology typical for immature oligodendrocytes, whereas wild-type cells did not (Figures 2A and 2C). qRT-PCR experiments confirmed the upregulation of MBP expression in $Ncor^{-/-}$ as compared to wild-type (WT) NSCs at the mRNA level (Figure 2D). These results indicate that NCOR plays a critical role in a repression checkpoint of OL differentiation in embryonic multipotent NSCs and that absence of NCOR initiates specification into OL cell types.

HDAC Inhibitors Promote OL Differentiation in Combination with T3 Stimulation, but Not Alone

NCOR was originally identified as interacting with the unliganded T3 receptor (T3R) to repress gene transcription. Indeed, it has been firmly established that T3 stimulation leads to transcriptional activation of its target genes by initiating removal of transcriptional corepressors such as NCOR from T3R, resulting in recruitment of coactivator proteins (Astapova et al., 2008; Hermanson et al., 2002a; Perissi et al., 2010). As T3 plays an essential role during OL development (Billon et al., 2002), and can lead to the specification of embryonic NSCs into the oligodendrocyte lineage (Johe et al., 1996), we reasoned that NCOR may repress OL differentiation through its role as a T3R corepressor. Treatment of wild-type embryonic NSCs with T3 induced OL differentiation in NSC cultures, as assessed by morphology and the upregulation of OL-characteristic genes, including *Mbp* and *Plp*, and early immunocytochemical markers, including RIP, at both the mRNA and protein level (Figures 2E and 2F), in accordance with previous reports (Johe et al., 1996).

While conventional models would associate NCOR-mediated repression with HDAC repressor function, alleviation of HDAC activity has paradoxically mostly been associated with inhibition of OL differentiation (Figure S2A) (Copray et al., 2009; Marin-Husstege et al., 2002; Ye et al., 2009), suggesting that HDACs are rather required for OL differentiation. To investigate whether T3 modulated the effects of HDAC inhibition on the OL lineage,

(B) qPCR analysis of regions in the vicinity of *Sox8* and *Pax6* after ChIP for HDAC2 and HDAC3 in NSCs.
(C) Immunoblotting of NSC protein lysates with antibodies to class I HDAC proteins. Molecular weights (approximately): HDAC1 and HDAC2, 60 kDa; HDAC3, 50 kDa.
(D) Quantification of the numbers of TuJ1-positive cells after treatment with control siRNA (siECFP), siHDAC2, siHDAC3, and siHDAC2+3.
(E) Immunofluorescence micrographs depicting NSCs stained for acetylated H3K9 after treatment with siECFP, siHDAC2, siHDAC3, and siHDAC2+3.
(F) qPCR of the *Bdnf IV* promoter following ChIP with anti-acetyl-H3K9 and anti-acetyl-H3K14 antibodies following transfection of control (siECFP) or *Hdac3* siRNA.
(G) qRT-PCR analysis of *Bdnf* mRNA levels following transfection with siECFP, siHDAC2, or siHDAC3.
(H) qRT-PCR analysis of *Bdnf* mRNA levels in NSCs cultured from wild-type or $Smrt^{-/-}$ embryos.
(I) qPCR of the *Bdnf IV* promoter following ChIP with anti-SMRT and anti-HDAC3 antibodies in NSCs.
The scale bar represents 40 μm (E). All experiments were performed in n = 3–5 independent experiments, *p < 0.05, **p < 0.01 (t test). Error bars, SEM.

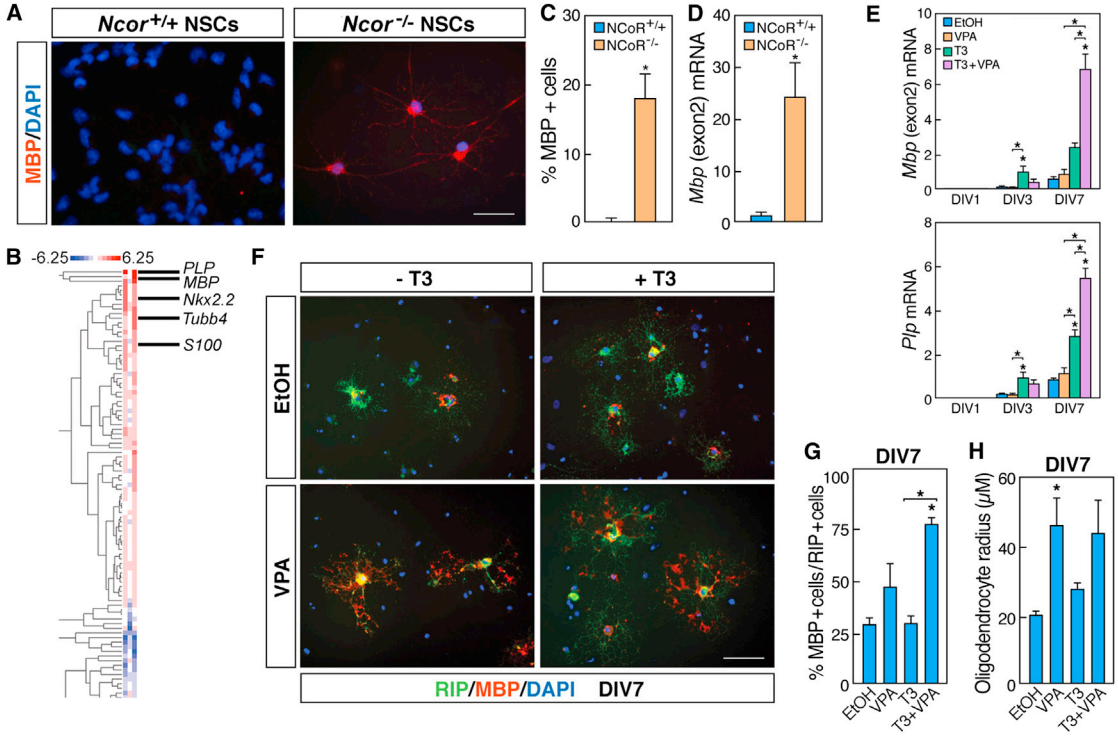

Figure 2. *Ncor*$^{-/-}$ NSCs Differentiate into Oligodendrocyte-like Cells Similar to T3 Treatment, and the HDAC Inhibitor VPA Enhances the T3-Mediated Differentiation

(A) Micrographs depicting NSCs isolated from wild-type (left panel) and *Ncor*$^{-/-}$ (right panel) embryos following immunocytochemistry with anti-MBP antibody (n = 3 independent experiments).

(B) RNA profiling data from *Ncor*$^{-/-}$ NSCs after 4 DIV, displaying the enrichment of increased expression of oligodendrocyte-associated genes (n = 3 independent samples).

(C) Quantification of MBP-positive cells in WT or *Ncor*$^{-/-}$ NSCs at 4 DIV (n = 3–5 independent experiments).

(D) qRT-PCR analysis of *Mbp* mRNA levels in wild-type or *Ncor*$^{-/-}$ NSCs (n = 3–5 independent experiments).

(E) qRT-PCR analysis of *Mbp* and *Plp* mRNA levels in NSCs treated with T3 and/or VPA. (n = 5 independent experiments, all treatments compared in each day).

(F and G) Micrographs, and corresponding quantification, depicting expression of RIP (green) and MBP (red) proteins in NSCs following treatment with T3 and/or VPA (n = 3 independent experiments). 20× objective.

(H) Quantification of oligodendrocyte radius following treatment of NSCs with T3 and/or VPA (n = 4 independent experiments, compared to EtOH treatment).

Scale bars represent 40 μm (A) and 80 μm (F). Statistical analysis: one-way ANOVA analysis of variance with Bonferroni's multiple comparison test except (C) and (D) (t test); *p < 0.05. Error bars, SEM.

embryonic NSCs were treated with T3 and VPA (0.5 mM), either alone or in combination. While T3 alone resulted in promotion of OL differentiation and gene expression, the expression of OL genes did not change in response to VPA alone (Figure 2E). In contrast, cotreatment of the NSCs with both T3 and VPA resulted in increased expression of *Mbp* and *Plp* after 7 DIV (Figure 2E). We also observed an increase in late markers of OL differentiation as compared to early markers in cells treated with both T3 and VPA at 7 DIV. Specifically, we found an increase in the number of cells displaying the late marker MBP double labeled with the early OL marker RIP, from 29% ± 3.2 in control conditions to 77% ± 3.4 in T3+VPA conditions (Figures 2F and 2G). In accordance with the increased MBP/RIP ratio and the possible increase in maturation, T3+VPA cotreatment resulted in morphological signs of late OL differentiation, including formation of myelin plaque-like structures (Figure 2F) and an increase in the average oligodendrocyte radius (Figure 2H). Notably, VPA treatment alone increased MBP immunoreactivity and the average oligodendrocyte radius in a very small subset of cells (Figure 2G and 2H), but it had no effect compared to the vehicle (EtOH) on the actual number of immature oligodendrocytes (Figures S2B and S2C).

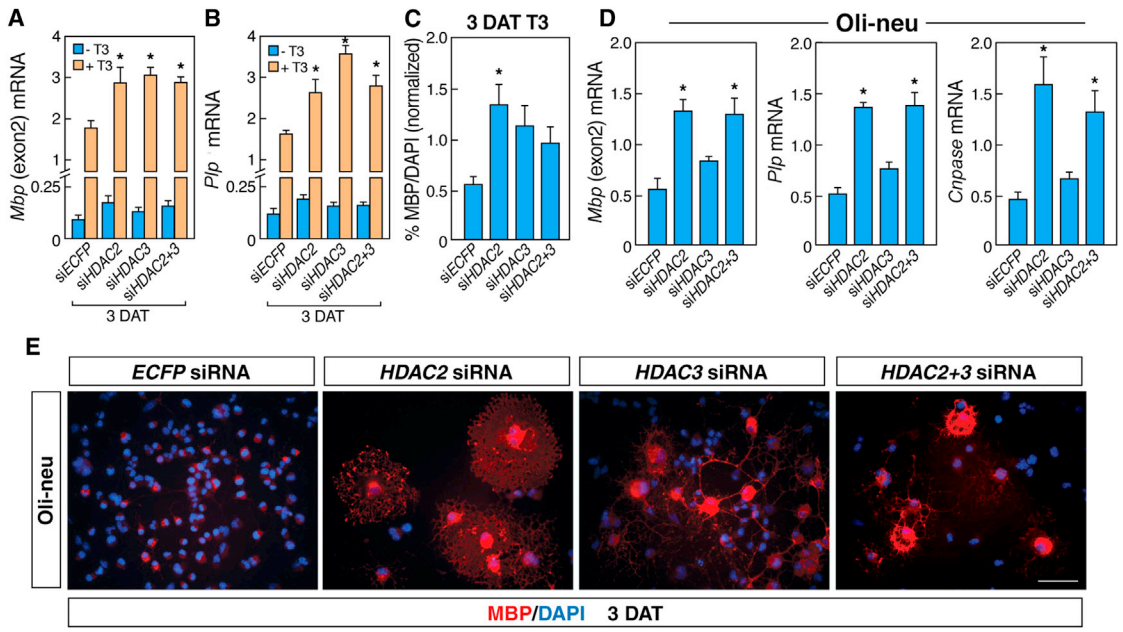

Figure 3. HDAC2 Regulates T3-Enhanced Oligodendrocyte Differentiation in NSCs

(A and B) qRT-PCR analysis demonstrating the effects of *Hdac2* and/or *Hdac3* siRNAs on *Mbp* and *Plp* mRNA levels in NSCs before and after T3 treatment (n = 4 independent experiments).

(C) Quantification of NSCs positive for MBP following transfection with control siRNA (ECFP) or siRNAs to *Hdac2* and/or *Hdac3* in the presence or absence of T3 relative to nuclear DAPI staining (n = 4 independent experiments).

(D) qRT-PCR results demonstrating the effects of *Hdac2* and/or *Hdac3* siRNAs on *Mbp*, *Plp*, and *Cnpase* mRNA levels in Oli-neu cells (n = 7, compared to *ECFP* siRNA).

(E) Immunocytochemistry of treated Oli-neu cells with MBP antibody (in red) and with DAPI (blue) counterstain.

All experiments: n = 3–5 independent experiments. Scale bars represent 80 μm (E). Statistical analysis: one-way ANOVA analysis of variance with Bonferroni's multiple comparison test; *p < 0.05. Error bars, SEM.

HDAC2 Mediates Specific Control of *Sox10* Expression in OL Differentiation

The ChIP-seq analysis revealed binding of HDAC2 to a subset of genes associated with oligodendrocyte differentiation, including *Sox8*, suggesting that HDAC2 might play a role in the oligodendrocyte lineage. Thus, we differentiated NSCs in the presence or absence of T3 for 3 days, lipofected the cells with siRNAs against *Hdac2* and/or *Hdac3*, and then assessed the OL differentiation at 3 days after siRNA transfection (DAT) (see Figure S2D for scheme). In the absence of T3, no significant effects on the expression of genes associated with OL and glial development were seen after siRNA knockdown of *Hdac2* or *Hdac3* alone or in combination at 3 DAT (Figures 3A and 3B; data not shown). However, in the presence of T3, there was a significant upregulation of MBP and PLP expression following transfection with siHDAC2 or siHDAC3 (Figures 3A–3C), although we noted that the predominant effects on the expression of these genes were mediated by T3. Moreover, knockdown of *Hdac2* but not *Hdac3* in the oligodendrocyte cell lines Oli-neu (Jung et al., 1995) and CG4 (Louis et al., 1992) also induced an increased expression of oligodendrocyte markers as MBP, CNPase, and PLP (Figures 3D and 3E; Figures S3A, S3B, and S3H), which in the Oli-neu cells was accompanied by a dramatic change of morphology (Figure 3E; Figure S3A). These results suggest that the effects of VPA on OL differentiation by T3 are at least partially dependent on HDAC2 activity.

We next performed a functional screen to compare gene expression profiles of T3-treated NSCs to NSCs treated with VPA only or with VPA+T3, with particular attention to genes implicated in glial differentiation. While the expression of many OL-characteristic genes were influenced by T3 but not VPA, expression of the OL-associated transcription factor *Sox10* was specifically increased 4-fold after VPA and VPA+T3 treatment, but unaffected by T3 alone (Figure 4A). Interestingly, *Sox10* expression was increased by siHDAC2 upon T3 treatment (Figure 4B). In contrast, *Sox10* mRNA levels were not affected by siHDAC3, by T3 treatment, or in *Ncor*$^{-/-}$ or *Smrt*$^{-/-}$ NSCs (Figures 2B, 4A, and 4B; Jepsen et al., 2007). In accordance with this result, *Sox10* mRNA levels were also increased upon *Hdac2*, but not *Hdac3* knockdown in Oli-neu cells (data not shown; see further below). A similar trend was seen for *Sox8*, detected as a

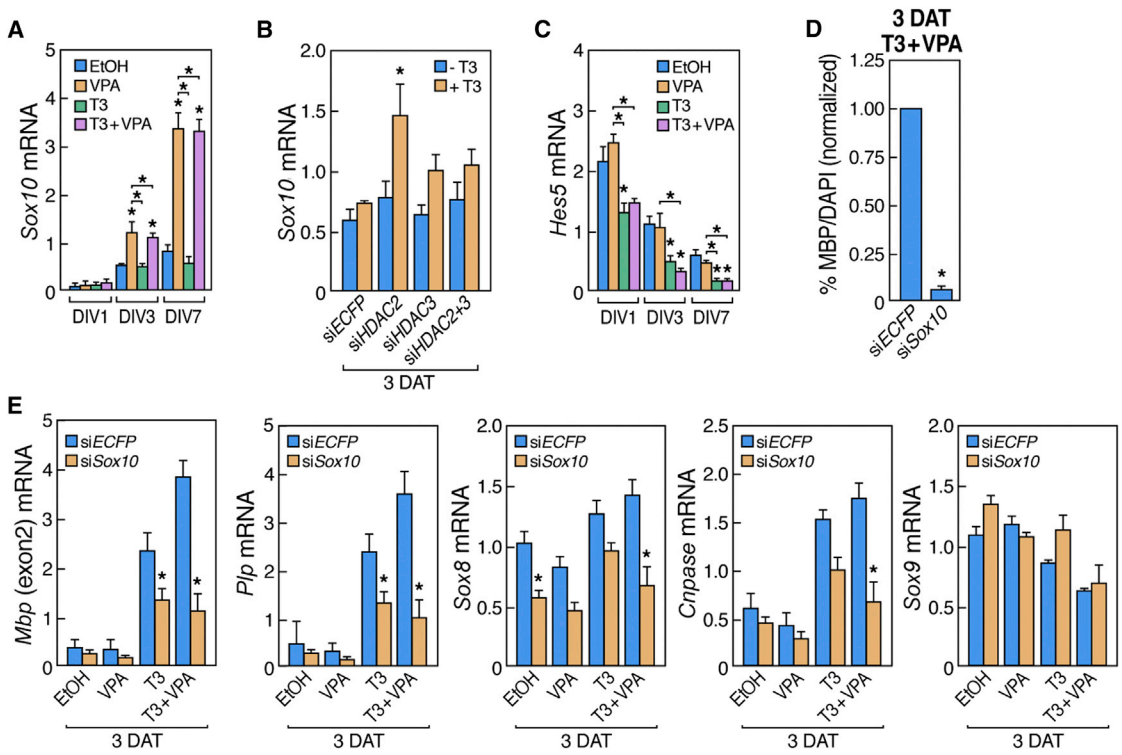

Figure 4. HDAC2 Regulates *Sox10* Expression, and *Sox10* Knockdown in NSCs and Oli-neu Cells Prevents Effects of T3 and VPA on Oligodendrocyte Differentiation

(A) qRT-PCR analysis of *Sox10* mRNA levels in NSCs treated with T3 and/or VPA.

(B) qRT-PCR analysis of *Sox10* mRNA levels in NSCs transfected with control siRNA (ECFP) or siRNAs to *Hdac2* and/or *Hdac3* in the presence or absence of T3.

(C) qRT-PCR analysis of *Hes5* mRNA levels in NSCs treated with T3 and/or VPA.

(D) Quantification of NSCs expressing MBP following transfection with control siRNA (ECFP) or *Sox10* siRNAs in the presence of T3 and VPA relative to nuclear DAPI staining.

(E) qRT-PCR demonstrating the effects of *Sox10* siRNA on expression of *Mbp*, *Plp*, *Sox8*, *Cnpase*, and *Sox9* following VPA and/or T3 treatment.

All experiments: n = 3–5 independent experiments. Statistical analysis: one-way ANOVA analysis of variance with Bonferroni's multiple comparison test; *p < 0.05. Error bars, SEM.

direct HDAC2 target in the ChIP-seq experiments (Figure 1B). Transcriptional inhibitors of OL differentiation, such as *Hes5*, were not affected by treatment with VPA alone in the NSCs (Figure 4C), in contrast to what has been observed in postnatal oligodendrocyte precursor cells (OPCs) (Lyssiotis et al., 2007; Shen et al., 2008).

SOX10 is required for terminal OL differentiation as null mutant mice for this SoxE protein generate normal numbers of OL progenitors that fail to terminally differentiate (Stolt et al., 2002). To test whether SOX10 could mediate the additive effects of VPA in T3-mediated OL differentiation of embryonic NSCs, NSCs were differentiated in the presence of VPA and/or T3 and lipofected at 3 days with siRNA against *Sox10* (Roh et al., 2006) (Figure S2D; Figure S1B for efficiency of the siRNA). Gene expression was then analyzed 3 DAT. Knockdown of *Sox10* partially prevented the upregulation of MBP and PLP and blocked the terminal OL differentiation induced by the cotreatment of VPA and T3 at 3 DAT (Figures 4D and 4E). *Sox10* knockdown also reduced the mRNA levels of *Cnpase* and *Sox8* at 3 DAT, but importantly did not affect earlier markers, including *Sox9*, in differentiating NSCs (Figure 4E). We conclude that SOX10 is required for the proper OL differentiation effects observed when treating NSCs with VPA or siHDAC2 and T3.

To investigate specific roles for class I HDACs in the VPA-mediated potentiation of OL differentiation of NSCs, we next investigated the presence of HDAC2 and HDAC3 at previously characterized regulatory regions of *Mbp* (Farhadi et al., 2003) and *Sox10* (Werner et al., 2007) in the embryonic NSCs (Figure 5A). ChIP-qPCR analysis indicated that while both HDAC2 and HDAC3 were present in the

regulatory regions of the *Mbp* gene in NSCs and Oli-neu cells (Figure 5B; Figure S3D), HDAC2 was specifically enriched in the U2 enhancer of *Sox10* (Figure 5B, left panel). This HDAC2 enrichment was observed both in comparison to other regions bound by HDAC2 as well as in comparison to the occupancy of HDAC3 at the same region (Figure 5B). Similar results were obtained in Oli-neu cells (Figures S3C and S3F). Indeed, an analysis of the acetylation state of the regulatory regions of *Sox10* revealed relatively low acetylation levels of H3K14 and H4K16, but not H3K9, at the U2 enhancer in NSCs and to an extent also in the Oli-neu cells, strengthening the observation of increased HDAC2 occupancy at this specific enhancer (Figure 5C; Figure S3E). The U2 enhancer is an element that previously has been shown to regulate *Sox10* expression specifically in the oligodendrocyte lineage starting at embryonic midgestation (Küspert et al., 2011; Werner et al., 2007). Together with our data, this suggests that HDAC2 may be specifically required for *Sox10* gene regulation in early oligodendrocyte development. Class I HDACs and NCORs have been identified as binding partners of SOX2 (Engelen et al., 2011), and an in silico analysis revealed a putative binding site for SOX2 in the U2 enhancer of *Sox10* (Figure S4). We therefore investigated whether this T3 and NCoR-independent HDAC2-mediated repression of *Sox10* could be mediated in association with SOX2. Indeed, we found a significant enrichment of SOX2 occupancy on the U2, but not U1, enhancer compared to control regions (Figure 5D; data not shown). siRNA-mediated knockdown of *Sox2*, however, did not result in any significantly increased expression of *Sox10* (data not shown), suggesting that other factors are sufficient to recruit HDAC2 to the U2 enhancer and mediate the essential repression.

Sox10, but Not HDACs, Is Required for Maintenance of the Differentiated State in Postnatal OL Progenitors

The differentiation of OPCs begins in early postnatal stages in the forebrain, although its peak occurs a few days later (Wegner, 2008). It is noteworthy that *Hdac2* expression has been reported to decrease in cells of the oligodendrocyte lineage at these stages (Shen et al., 2005). Interestingly, we did not observe any morphological signs of premature differentiation of the proliferating postnatal CG4 upon siHDAC2 and/or siHDAC3 delivery (data not shown), in contrast to what we observed in embryonic Oli-neu cells or T3-treated NSCs (Figure 2; Figure S3A). Moreover, although moderate increases in gene expression levels of *Mbp* and *Plp* were observed following transfection with siHDAC2 in the CG4 cells (Figure S3H), these were found not to be associated with an siHDAC2-mediated *Sox10* derepression as *Sox10* levels were indeed rescued by siHDAC2, but *Mbp* and *Plp* expression levels were not in these cells (Figure S3H; data not shown). These results suggested that SOX10 could play alternative roles at this late stage of OL differentiation. Intriguingly, *Sox10* siRNA delivery at this stage instead resulted in a dramatic increase in gene expression associated with the stem cell state (Pevny and Nicolis, 2010; Scott et al., 2010), including *Sox2*, *Sox9*, *Sox8*, and *Hes5*, without affecting markers of neuronal differentiation (Figure 5E; data not shown). This result stands in sharp contrast to the mild effects of *Sox10* siRNA on the expression of these genes in NSCs and a reversible increase of *Sox9* expression in Oli-neu cells (Figure 4E; data not shown). Taken together, our observations suggest that *Sox10* expression is required for efficient progression of oligodendrocyte differentiation and expression of late OL characteristic genes and at a later stage serves to maintain the differentiated state and suppress the expression of genes associated with more undifferentiated progenitors and stem cells (Figure 6).

DISCUSSION

Transcriptional corepressors such as NCOR and SMRT have distinct roles in repressing differentiation in NSCs, and we therefore hypothesized that associated HDACs also have specific functions albeit the reports so far have been unclear. Here we demonstrate that whereas HDAC3 and SMRT, and not HDAC2 or NCoR, are part of a repression checkpoint for neuronal differentiation in embryonic NSCs, NCoR and HDAC2 constitute specific repressor checkpoints in control of oligodendrocyte differentiation (Figure 6). The mechanism by which HDAC2 inhibits oligodendrocyte differentiation is at least in part, via repression of the key transcription factor SOX10, coinciding with binding of HDAC2 to the SOX2-occupied U2 enhancer of the *Sox10* gene (Figure 6). Together, these data reveal nonredundant roles for class I HDACs and associated factors in NSC differentiation.

Our results suggest that specific HDACs play distinct roles in the differentiation of NSCs. Chemical or genetic ablation of class I HDAC activity have been reported to inhibit oligodendrocyte and Schwann cell differentiation and promote neuronal differentiation (Copray et al., 2009; Hsieh et al., 2004; Marin-Husstege et al., 2002). In these studies, HDACs are suggested to repress inhibitors of OL differentiation, thereby being required for proper oligodendrocyte differentiation. However, deletion of the HAT CREB-binding protein also results in decreased oligodendrocyte differentiation and corpus callosum deficits (Wang et al., 2010), and HDACs have also been shown to be required for neurogenesis (Montgomery et al., 2009), blurring a general consensus statement of the function of these factors in NSC differentiation. In the present study, loss of HDAC2 activity in the presence of T3 resulted in enhanced oligodendrocytic

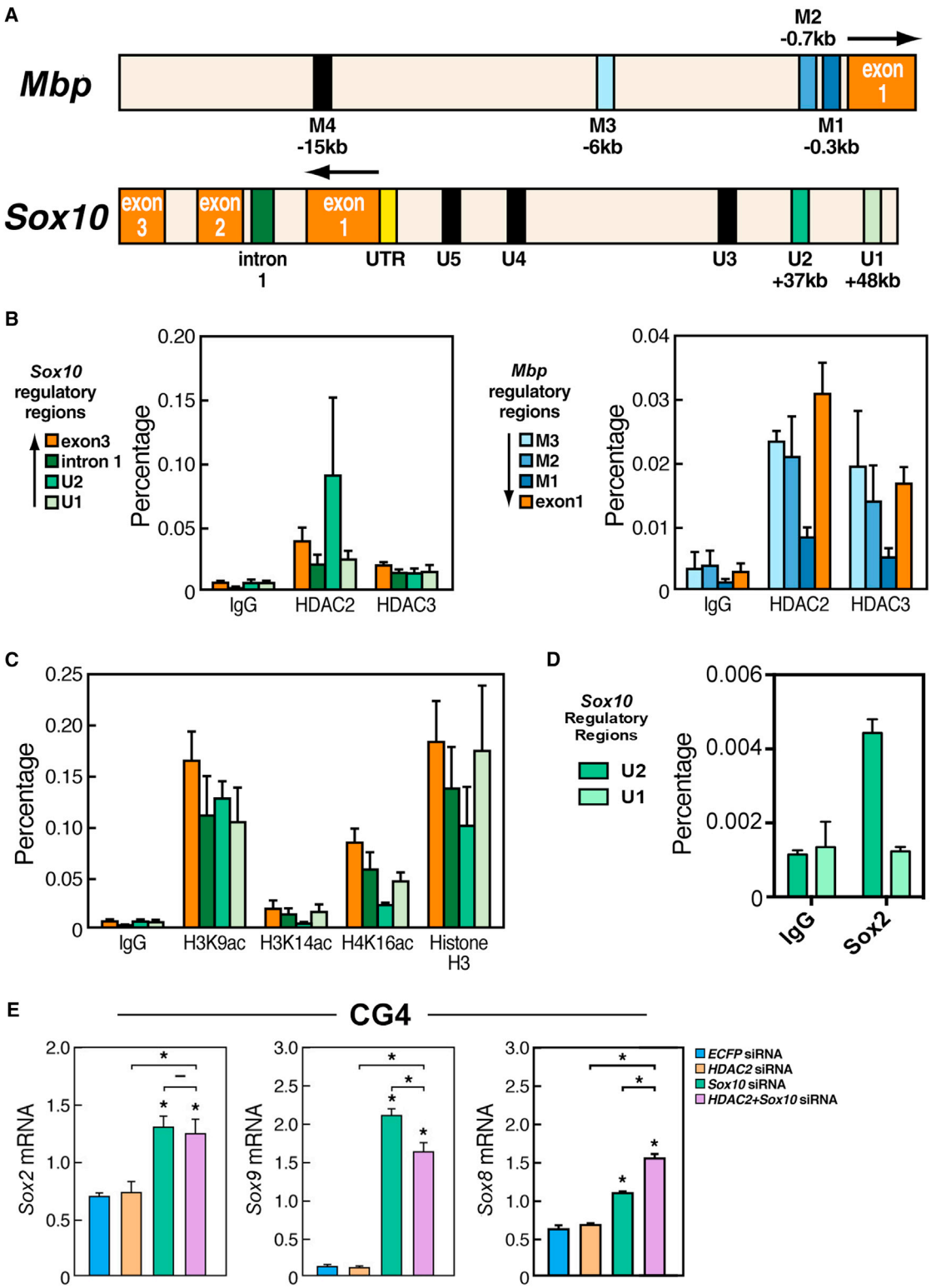

Figure 5. HDAC2 Occupies Developmentally Critical Regulatory Regions of *Sox10* in NSCs, and *Sox10* Controls a More Mature Signature of Postnatal Oligodendrocyte Precursors by Repression of *Sox2* and *Sox9*

(A) Diagram depicting some of the regulatory regions of *Mbp* (M1-M4) and *Sox10* (U1-U5) and their distance to the transcription start site.

(B) qPCR analysis of the indicated regions of *Sox10* and *Mbp* following ChIP of HDAC2 or HDAC3. Percentage, percentage of input (1%).

(legend continued on next page)

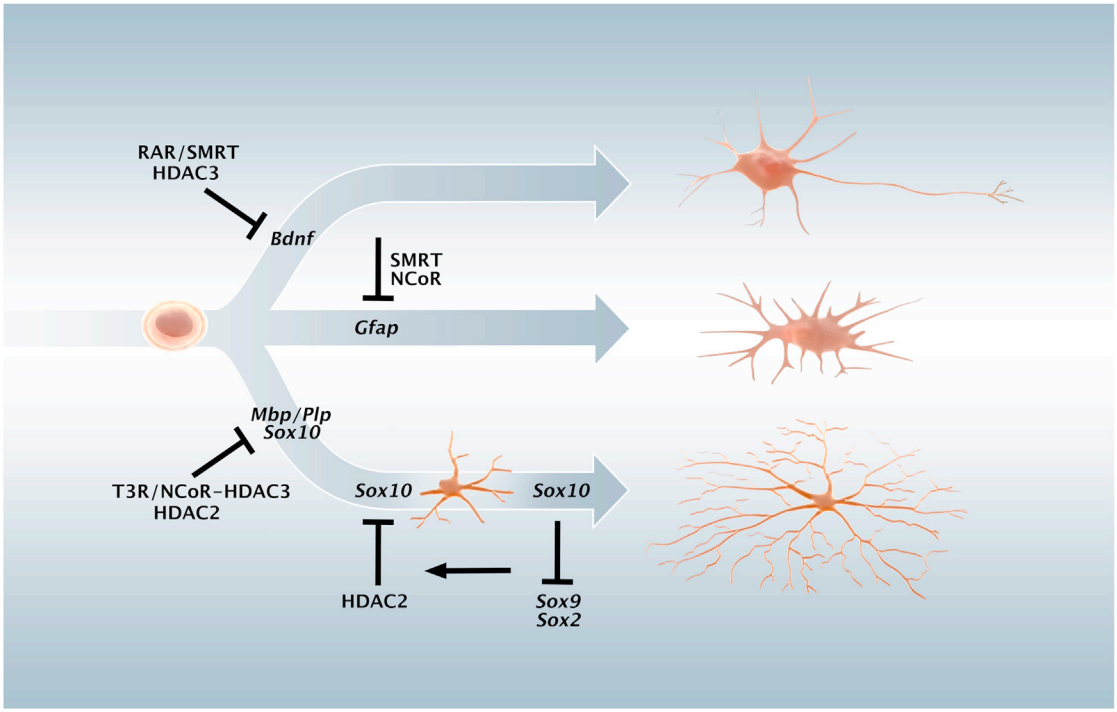

Figure 6. NCOR and HDACs Play Nonredundant Roles in the Regulation of Neural Stem Cell Differentiation

In multipotent embryonic NSCs, SMRT and HDAC3 are nonredundantly repressing neuronal differentiation, at least in part by repressing *Bdnf* expression required for the cell survival during the progression of neuronal differentiation. Astrocytic differentiation is repressed by both NCOR and SMRT. Oligodendrocyte differentiation is repressed by NCOR and HDAC2 in neural stem cells by repressing different OL-associated genes. In Oli-neu cells (prenatal oligodendrocyte progenitors), a repression of *Sox10* is maintained by HDAC2 that occupies the regulatory U2 enhancer of *Sox10*. In CG4 cells (postnatal oligodendrocyte precursors), *Sox10* is not only required for the progression of OL differentiation but also for retaining a more differentiated state by being required for efficient repression of *Sox2* along with *Sox9*, *Hes5*, and other progenitor associated genes.

differentiation in embryonic cortical NSCs. Strikingly, HDAC2 does repress directly the key OL transcription factor *Sox10*, in contrast to the indirect effects of HDACs previously reported. Thus, the effects of HDAC inhibition on NSCs appear to be distinct depending on cell-type specificity, the temporal window of action, and the presence of additional factors. These cell-type and temporal specific effects of HDACs are in line with what has been reported for components of the NOTCH and WNT signaling, which can have both repressing and activating functions in oligodendrocyte development (Popko, 2003; Tawk et al., 2011).

Class B1 Sox proteins such as SOX2 are established repressors of differentiation and required to retain stem cell characteristics during development and in the adult (Arnold et al., 2011; Bylund et al., 2003; Engelen et al., 2011; Graham et al., 2003), but it has been shown that SOX2 can also act as a transcriptional activator in certain developmental contexts (Hoffmann et al., 2014). Our data on NCOR, HDAC2, and SOX10 suggest a transcriptional "transmission" mechanism where the appropriate "gear" controls the level of progenitor state and early and late progression of oligodendrocyte differentiation. In NSCs and embryonic OPCs, HDAC2 were found to bind to the critical U2 enhancer regulating *Sox10* in association with SOX2, and alleviation of HDAC2 led to an increase in *Sox10* expression. OLIG2 has recently been shown to

(C) qPCR of the indicated regions of *Sox10* following ChIP of acetylated H3K9, H3K14, or H4K16 from NSCs. Histone H3 is shown as a control for ChIP efficiency.
(D) qPCR of the indicated regions after ChIP of SOX2 revealed that SOX2 is bound to the U2, but not the U1, enhancer of the *Sox10* gene.
(E) qRT-PCR demonstrating the effects of *Sox10* siRNA and/or *Hdac2* siRNA on the expression of *Sox2*, *Sox8*, and *Sox9* in CG4 cells (postnatal OPCs) after *Sox10* RNA knockdown.
All experiments: n = 2–3 independent experiments. Statistical analysis: one-way ANOVA analysis of variance with Bonferroni's multiple comparison test; *p < 0.05. Error bars, SEM.

activate the U2 enhancer (Küspert et al., 2011) and as such could also be a candidate for the upregulation of *Sox10* expression. Nevertheless, in contrast to SOX2 (Figure 5D), OLIG2 is present not only at the U2 enhancer in immature oligodendrocytes but also at the U1, U3, U4, and U5 *Sox10* enhancers (Yu et al., 2013), suggesting a more general role in the transcriptional regulation of SOX10. While OLIG2 is an important regulator of this system, we do not observe an upregulation of *Olig2* upon VPA+T3 treatment or *Hdac2* and/or *Hdac3* siRNA in NSCs and Oli-neu cells, respectively (Figures S3G and S3I). It will be of immediate interest to elucidate additional factors responsible for HDAC2 recruitment to the U2 enhancer in NSCs and prenatal oligodendrocyte progenitors. Indeed, since *Sox2* knockdown failed to induce a significant increase in *Sox10* expression even in the presence of T3, it is plausible that other class B1 Sox factors such as SOX1/3 could be involved, and the role for class B2 factors binding similar sequences but with alternative actions, such as SOX14 or SOX21, should be further investigated.

In postnatal OPCs, increased levels of SOX10 seem to repress *Sox2* expression and consequently promote late progression of oligodendrocyte differentiation. Intriguingly, forced *Sox2* expression mediates dedifferentiation of maturely differentiated oligodendrocytes (Kondo and Raff, 2000, 2004) and SOX9 has been shown to promote neural stem cell state (Scott et al., 2010). Whereas there are few previous demonstrations of such key factors maintaining differentiated state in the central nervous system, the requirement of SOX10 for retaining a more differentiated state partly resembles the master role of PAX5 maintaining the differentiated state of mature B lymphocytes (Cobaleda et al., 2007). Our present observations that SOX10 is required for repression of *Sox2* and *Sox9* in late oligodendrocyte precursor cells, in addition to the distinct requirements for NCOR, SMRT, and HDAC-regulated repressor actions in the progression of neural stem and progenitor differentiation, suggest a distinct order of repressor and corepressor action to mediate the serial events that details the neuronal and oligodendrocyte lineages, with expression of *Sox10* required to prevent reexpression of gene products promoting stem cell characteristics.

EXPERIMENTAL PROCEDURES

Embryonic Neural Stem Cell Cultures

Rat embryonic neural stem cells were derived as previously described in detail elsewhere (Hermanson et al., 2002a; Johe et al., 1996; Joseph et al., 2009). In brief, rat cortical tissue from embryonic day 15.5 was dissociated and 800 × 10^3 cells were plated per 10 cm dish, previously coated with poly-L-ornithine and fibronectin (both from Sigma-Aldrich). Neural stem cells were then expanded in N2 media with 10 ng/ml of basic fibroblastic growth factor (R&D Systems) and passaged by light dissociation in the presence of HBSS, NaHCO3, and HEPES (from Invitrogen and Sigma-Aldrich). For differentiation assays, neural stem cells (passage 1) were plated at the following densities: 150 × 10^3 cells in 35 mm plates (Corning) or 300 × 10^3 cells in 60 mm plates (Corning). NSCs were differentiated for up to 7 DIV in the absence of FGF-2 (N2), in the presence of VPA (0.5 mM, a concentration at which it specifically inhibits class I HDACs, Sigma-Aldrich) (Göttlicher et al., 2001) or its vehicle 70% ethanol (EtOH), and with or without thyroid hormone (T3—50 ng/ml, Sigma-Aldrich). Factors were added daily and media was changed every second day. After 1, 3, or 7 DIV, cells were fixed with 10% formalin (Sigma-Aldrich) and analyzed by immunocytochemistry or qRT-PCR. For ChIP assays, NSCs were expanded after the first passage until confluency, without contact between adjacent colonies. Animals were treated in accordance with institutional and national guidelines, with all required ethical permits. In Figure S2, FGF2 (10 ng/ml) expanded NSCs were treated for 3 DIV with FGF2 (10 ng/ml), IGF-2 (5 ng/ml), and PDGF-BB (10 ng/ml) (OPC media).

OPC Cultures

The embryonic OPC cell line Oli-neu and the postnatal OPC cells were cultured as previously described (Jung et al., 1995; Louis et al., 1992); for details see Supplemental Information.

Transfection-Lipofection

siRNAs or pcDNAEF1-eGFP (Amaxa) were lipofected using Lipofectamine 2000 (Invitrogen), following the manufacturer's instructions. Three micrograms of siRNA or 1 μg pcDNAEF1-eGFP was used per 35-mm plate. Opti-MEM I reduced serum medium was used to prepare the complexes. Cells were changed to Dulbecco's modified Eagle's medium (Invitrogen) and incubated with the complexes for 4 hr before returning to their original media. Cells were collected for immunocytochemistry or qRT-PCR analysis after 1 or 3 DIV. Lipofection of siRNA in differentiated conditions was performed after 3 DIV differentiation. The following target sequences for siRNAs (A4 synthesis, Dharmacon) were used.

ECFP Control

5′-GAAGAACGGCAUCAAGGCC-3′.

Sox10

5′- CUGCUGUUCCUUCUUGACC-3 (Roh et al., 2006).

Hdac2

(1) 5′-AAA UGU CGC UGA UCA UAA GAA-3′.
(2) 5′-AAG GUG UUC AAA UGC AAG CUA-3′.

Hdac3

(1) 5′-AAU AGC CUA GUC CUG CAU UAU-3′.
(2) 5′-AAC ACA GCU AAA CAA UAA GAU-3′

Optimal results for differentiation and gene expression in NSCs by HDAC2 and HDAC3 siRNAs were titrated to knockdowns in the range of 50%–75%. Higher efficiency resulted in increased cell death along with previous observations, and lower efficiency yielded less significant results.

Chromatin Immunoprecipitation and qPCR

ChIP-IT Express (Active Motif) was used according to the supplier's recommendations. Cells were crosslinked using 1% formaldehyde for 10 min. Cells were rinsed twice with cold PBS, collected by

scraping and pelleted at 2,000 rpm for 4 min at 4°C. Frozen pelleted cells were resuspended in lysis buffer and centrifuged for 10 min at 4°C, and the pelleted nuclei were resuspended in the shearing buffer. Chromatin was then sonicated using a Bioruptor 200 (Diagenode) at high frequency, 0.5 min/0.5min, for 12 min. Sonicated chromatin was analyzed in a 3% agarose gel to confirm efficient sonication. Input was collected for further analysis. Five micrograms of chromatin was incubated for 1 hr at 4°C with protein G magnetic beads and then immunoprecipitated overnight at 4°C with the following antibodies: α-H3K9ac (07-352; Upstate, 5 μl), α-H3K14ac (06-911; Upstate, 5 μl), α-H4K16ac (07-329; Upstate, 5 μl), α-HDAC2 (sc-7899x; Santa Cruz, 5 μg), α-HDAC3 (sc-11417x; Santa Cruz, 5 μg), α-SOX2 (sc-17320x; Santa Cruz, 1 μg), RNA polymerase II (Active Motif, positive control for ChIP-IT Express, 2 μg), Histone H3 (Abcam, ab1791, 2 μg), rabbit IgG (Active Motif, negative control, 2 μg; Santa Cruz, sc-2027, 1 μg), and goat IgG (Santa Cruz, sc-2028, 1 μg). After three washes with ChIP buffer 1 and two washes with ChIP buffer 2, the IP DNA was reverse crosslinked and resuspended in a final volume of 130 μl. Purified DNA and 1% input were analyzed by qPCR, using 5-fold dilutions of the input for standard curves and triplicates per sample. When primer dimers were detected, the relative quantity for the specific sample was considered to be zero. As the standard curve method was used, potential differences in primer efficiency were taken in account and occupancy in different regulatory regions could be compared for a specific antibody.

RNA Profiling

RNA profiling was performed as previously described (Jepsen et al., 2007); for details see Supplemental Information.

Statistical Analysis

Statistical analysis and graphs were performed using the software Prism 4 (Graph Pad). When comparing to a hypothetical control value (100%), one sample t test was used. When two groups were compared, statistical analysis was performed using two-tailed unpaired t test. When comparing three or more groups, one-way ANOVA analysis of variance with Bonferroni's multiple comparison test was used. Comparisons were performed between all treatments, unless stated otherwise. The threshold value for statistical significance (α value) was set at 0.05 (*$p < 0.05$). In all graphs, results are expressed as mean ± SEM. The "n" in the figure legends represents the number of independent experiments.

ACCESSION NUMBERS

The ChIP-seq data are freely accessible in the GEO database under accession number GSE57232. Additional descriptions of qRT-PCR, immunocytochemistry and ChIP-seq methods can be found in the Supplemental Information.

SUPPLEMENTAL INFORMATION

Supplemental Information includes Supplemental Experimental Procedures, four figures, and one table and can be found with this article online at http://dx.doi.org/10.1016/j.stemcr.2014.07.008.

ACKNOWLEDGMENTS

We would like to thank Dr. J.C. Louis (Amgen) for the CG4 cell line (Louis et al., 1992), Dr. J. Trotter (University of Mainz) for the Oli-neu cell line (Jung et al., 1995), J. Hightower for artwork, and Dr. M. Götz and members of the O.H. lab for valuable discussions. M.G.R. is a Howard Hughes Medical Institute Investigator. This study was supported by NIH grants (to M.G.R.), a Scientist Development Grant from the American Heart Association (to K.J.), and grants from the Swedish Brain Foundation (Hjärnfonden), David and Astrid Hagélen Foundation, SSMF (Svenska Sällskapet för Medicinsk Forskning), the Marie Curie Integration Grant, Seventh Framework Programme, European Union (to G.C.-B.), the Swedish Research Council (VR-MH), Karolinska Institutet Research Foundations, the Swedish Society of Medicine (SLS) (to G.C.-B. and O.H.), the Swedish Cancer Society (CF), the KI Cancer Network, the Swedish Foundation for Strategic Research (SSF), and the Swedish Childhood Cancer Foundation (BCF) (to O.H.).

Received: June 20, 2013
Revised: July 20, 2014
Accepted: July 21, 2014
Published: August 28, 2014

REFERENCES

Andreu-Agulló, C., Morante-Redolat, J.M., Delgado, A.C., and Fariñas, I. (2009). Vascular niche factor PEDF modulates Notch-dependent stemness in the adult subependymal zone. Nat. Neurosci. *12*, 1514–1523.

Arnold, K., Sarkar, A., Yram, M.A., Polo, J.M., Bronson, R., Sengupta, S., Seandel, M., Geijsen, N., and Hochedlinger, K. (2011). Sox2(+) adult stem and progenitor cells are important for tissue regeneration and survival of mice. Cell Stem Cell *9*, 317–329.

Astapova, I., Lee, L.J., Morales, C., Tauber, S., Bilban, M., and Hollenberg, A.N. (2008). The nuclear corepressor, NCoR, regulates thyroid hormone action in vivo. Proc. Natl. Acad. Sci. USA *105*, 19544–19549.

Ballas, N., Grunseich, C., Lu, D.D., Speh, J.C., and Mandel, G. (2005). REST and its corepressors mediate plasticity of neuronal gene chromatin throughout neurogenesis. Cell *121*, 645–657.

Billon, N., Jolicoeur, C., Tokumoto, Y., Vennström, B., and Raff, M. (2002). Normal timing of oligodendrocyte development depends on thyroid hormone receptor alpha 1 (TRalpha1). EMBO J. *21*, 6452–6460.

Bylund, M., Andersson, E., Novitch, B.G., and Muhr, J. (2003). Vertebrate neurogenesis is counteracted by Sox1-3 activity. Nat. Neurosci. *6*, 1162–1168.

Cobaleda, C., Jochum, W., and Busslinger, M. (2007). Conversion of mature B cells into T cells by dedifferentiation to uncommitted progenitors. Nature *449*, 473–477.

Copray, S., Huynh, J.L., Sher, F., Casaccia-Bonnefil, P., and Boddeke, E. (2009). Epigenetic mechanisms facilitating oligodendrocyte development, maturation, and aging. Glia *57*, 1579–1587.

Covey, M.V., Streb, J.W., Spektor, R., and Ballas, N. (2012). REST regulates the pool size of the different neural lineages by restricting

the generation of neurons and oligodendrocytes from neural stem/progenitor cells. Development *139*, 2878–2890.

Engelen, E., Akinci, U., Bryne, J.C., Hou, J., Gontan, C., Moen, M., Szumska, D., Kockx, C., van Ijcken, W., Dekkers, D.H., et al. (2011). Sox2 cooperates with Chd7 to regulate genes that are mutated in human syndromes. Nat. Genet. *43*, 607–611.

Farhadi, H.F., Lepage, P., Forghani, R., Friedman, H.C., Orfali, W., Jasmin, L., Miller, W., Hudson, T.J., and Peterson, A.C. (2003). A combinatorial network of evolutionarily conserved myelin basic protein regulatory sequences confers distinct glial-specific phenotypes. J. Neurosci. *23*, 10214–10223.

Füllgrabe, J., Lynch-Day, M.A., Heldring, N., Li, W., Struijk, R.B., Ma, Q., Hermanson, O., Rosenfeld, M.G., Klionsky, D.J., and Joseph, B. (2013). The histone H4 lysine 16 acetyltransferase hMOF regulates the outcome of autophagy. Nature *500*, 468–471.

Göttlicher, M., Minucci, S., Zhu, P., Krämer, O.H., Schimpf, A., Giavara, S., Sleeman, J.P., Lo Coco, F., Nervi, C., Pelicci, P.G., and Heinzel, T. (2001). Valproic acid defines a novel class of HDAC inhibitors inducing differentiation of transformed cells. EMBO J. *20*, 6969–6978.

Graham, V., Khudyakov, J., Ellis, P., and Pevny, L. (2003). SOX2 functions to maintain neural progenitor identity. Neuron *39*, 749–765.

Heldring, N., Nyman, U., Lönnerberg, P., Onnestam, S., Herland, A., Holmberg, J., and Hermanson, O. (2014). NCoR controls glioblastoma tumor cell characteristics. Neuro-oncol. *16*, 241–249.

Hermanson, O., Glass, C.K., and Rosenfeld, M.G. (2002a). Nuclear receptor coregulators: multiple modes of modification. Trends Endocrinol. Metab. *13*, 55–60.

Hermanson, O., Jepsen, K., and Rosenfeld, M.G. (2002b). N-CoR controls differentiation of neural stem cells into astrocytes. Nature *419*, 934–939.

Hoffmann, S.A., Hos, D., Küspert, M., Lang, R.A., Lovell-Badge, R., Wegner, M., and Reiprich, S. (2014). Stem cell factor Sox2 and its close relative Sox3 have differentiation functions in oligodendrocytes. Development *141*, 39–50.

Hsieh, J., Nakashima, K., Kuwabara, T., Mejia, E., and Gage, F.H. (2004). Histone deacetylase inhibition-mediated neuronal differentiation of multipotent adult neural progenitor cells. Proc. Natl. Acad. Sci. USA *101*, 16659–16664.

Jepsen, K., Hermanson, O., Onami, T.M., Gleiberman, A.S., Lunyak, V., McEvilly, R.J., Kurokawa, R., Kumar, V., Liu, F., Seto, E., et al. (2000). Combinatorial roles of the nuclear receptor corepressor in transcription and development. Cell *102*, 753–763.

Jepsen, K., Solum, D., Zhou, T., McEvilly, R.J., Kim, H.-J., Glass, C.K., Hermanson, O., and Rosenfeld, M.G. (2007). SMRT-mediated repression of an H3K27 demethylase in progression from neural stem cell to neuron. Nature *450*, 415–419.

Johe, K.K., Hazel, T.G., Muller, T., Dugich-Djordjevic, M.M., and McKay, R.D. (1996). Single factors direct the differentiation of stem cells from the fetal and adult central nervous system. Genes Dev. *10*, 3129–3140.

Johnson, R., Teh, C.H., Kunarso, G., Wong, K.Y., Srinivasan, G., Cooper, M.L., Volta, M., Chan, S.S., Lipovich, L., Pollard, S.M., et al. (2008). REST regulates distinct transcriptional networks in embryonic and neural stem cells. PLoS Biol. *6*, e256.

Joseph, B., Andersson, E.R., Vlachos, P., Södersten, E., Liu, L., Teixeira, A.I., and Hermanson, O. (2009). p57Kip2 is a repressor of Mash1 activity and neuronal differentiation in neural stem cells. Cell Death Differ. *16*, 1256–1265.

Jung, M., Krämer, E., Grzenkowski, M., Tang, K., Blakemore, W., Aguzzi, A., Khazaie, K., Chlichlia, K., von Blankenfeld, G., Kettenmann, H., et al. (1995). Lines of murine oligodendroglial precursor cells immortalized by an activated neu tyrosine kinase show distinct degrees of interaction with axons in vitro and in vivo. Eur. J. Neurosci. *7*, 1245–1265.

Kondo, T., and Raff, M. (2000). Oligodendrocyte precursor cells reprogrammed to become multipotential CNS stem cells. Science *289*, 1754–1757.

Kondo, T., and Raff, M. (2004). Chromatin remodeling and histone modification in the conversion of oligodendrocyte precursors to neural stem cells. Genes Dev. *18*, 2963–2972.

Küspert, M., Hammer, A., Bösl, M.R., and Wegner, M. (2011). Olig2 regulates Sox10 expression in oligodendrocyte precursors through an evolutionary conserved distal enhancer. Nucleic Acids Res. *39*, 1280–1293.

Laeng, P., Pitts, R.L., Lemire, A.L., Drabik, C.E., Weiner, A., Tang, H., Thyagarajan, R., Mallon, B.S., and Altar, C.A. (2004). The mood stabilizer valproic acid stimulates GABA neurogenesis from rat forebrain stem cells. J. Neurochem. *91*, 238–251.

Lilja, T., Heldring, N., and Hermanson, O. (2013a). Like a rolling histone: epigenetic regulation of neural stem cells and brain development by factors controlling histone acetylation and methylation. Biochim. Biophys. Acta *1830*, 2354–2360.

Lilja, T., Wallenborg, K., Björkman, K., Albåge, M., Eriksson, M., Lagercrantz, H., Rohdin, M., and Hermanson, O. (2013b). Novel alterations in the epigenetic signature of MeCP2-targeted promoters in lymphocytes of Rett syndrome patients. Epigenetics *8*, 246–251.

Liu, X.S., Chopp, M., Kassis, H., Jia, L.F., Hozeska-Solgot, A., Zhang, R.L., Chen, C., Cui, Y.S., and Zhang, Z.G. (2012). Valproic acid increases white matter repair and neurogenesis after stroke. Neuroscience *220*, 313–321.

Louis, J.C., Magal, E., Muir, D., Manthorpe, M., and Varon, S. (1992). CG-4, a new bipotential glial cell line from rat brain, is capable of differentiating in vitro into either mature oligodendrocytes or type-2 astrocytes. J. Neurosci. Res. *31*, 193–204.

Lyssiotis, C.A., Walker, J., Wu, C., Kondo, T., Schultz, P.G., and Wu, X. (2007). Inhibition of histone deacetylase activity induces developmental plasticity in oligodendrocyte precursor cells. Proc. Natl. Acad. Sci. USA *104*, 14982–14987.

Marin-Husstege, M., Muggironi, M., Liu, A., and Casaccia-Bonnefil, P. (2002). Histone deacetylase activity is necessary for oligodendrocyte lineage progression. J. Neurosci. *22*, 10333–10345.

Miller, F.D., and Gauthier, A.S. (2007). Timing is everything: making neurons versus glia in the developing cortex. Neuron *54*, 357–369.

Montgomery, R.L., Hsieh, J., Barbosa, A.C., Richardson, J.A., and Olson, E.N. (2009). Histone deacetylases 1 and 2 control the

progression of neural precursors to neurons during brain development. Proc. Natl. Acad. Sci. USA *106*, 7876–7881.

Perissi, V., Jepsen, K., Glass, C.K., and Rosenfeld, M.G. (2010). Deconstructing repression: evolving models of co-repressor action. Nat. Rev. Genet. *11*, 109–123.

Pevny, L.H., and Nicolis, S.K. (2010). Sox2 roles in neural stem cells. Int. J. Biochem. Cell Biol. *42*, 421–424.

Popko, B. (2003). Notch signaling: a rheostat regulating oligodendrocyte differentiation? Dev. Cell *5*, 668–669.

Roh, J., Cho, E.A., Seong, I., Limb, J.K., Lee, S., Han, S.J., and Kim, J. (2006). Down-regulation of Sox10 with specific small interfering RNA promotes transdifferentiation of Schwannoma cells into myofibroblasts. Differentiation *74*, 542–551.

Ruthenburg, A.J., Li, H., Patel, D.J., and Allis, C.D. (2007). Multivalent engagement of chromatin modifications by linked binding modules. Nat. Rev. Mol. Cell Biol. *8*, 983–994.

Salminen, A., Tapiola, T., Korhonen, P., and Suuronen, T. (1998). Neuronal apoptosis induced by histone deacetylase inhibitors. Brain Res. Mol. Brain Res. *61*, 203–206.

Scott, C.E., Wynn, S.L., Sesay, A., Cruz, C., Cheung, M., Gomez Gaviro, M.V., Booth, S., Gao, B., Cheah, K.S., Lovell-Badge, R., and Briscoe, J. (2010). SOX9 induces and maintains neural stem cells. Nat. Neurosci. *13*, 1181–1189.

Shen, S., Li, J., and Casaccia-Bonnefil, P. (2005). Histone modifications affect timing of oligodendrocyte progenitor differentiation in the developing rat brain. J. Cell Biol. *169*, 577–589.

Shen, S., Sandoval, J., Swiss, V.A., Li, J., Dupree, J., Franklin, R.J., and Casaccia-Bonnefil, P. (2008). Age-dependent epigenetic control of differentiation inhibitors is critical for remyelination efficiency. Nat. Neurosci. *11*, 1024–1034.

Spivakov, M., and Fisher, A.G. (2007). Epigenetic signatures of stem-cell identity. Nat. Rev. Genet. *8*, 263–271.

Stolt, C.C., Rehberg, S., Ader, M., Lommes, P., Riethmacher, D., Schachner, M., Bartsch, U., and Wegner, M. (2002). Terminal differentiation of myelin-forming oligodendrocytes depends on the transcription factor Sox10. Genes Dev. *16*, 165–170.

Tawk, M., Makoukji, J., Belle, M., Fonte, C., Trousson, A., Hawkins, T., Li, H., Ghandour, S., Schumacher, M., and Massaad, C. (2011). Wnt/beta-catenin signaling is an essential and direct driver of myelin gene expression and myelinogenesis. J. Neurosci. *31*, 3729–3742.

Wang, J., Weaver, I.C., Gauthier-Fisher, A., Wang, H., He, L., Yeomans, J., Wondisford, F., Kaplan, D.R., and Miller, F.D. (2010). CBP histone acetyltransferase activity regulates embryonic neural differentiation in the normal and Rubinstein-Taybi syndrome brain. Dev. Cell *18*, 114–125.

Wegner, M. (2008). A matter of identity: transcriptional control in oligodendrocytes. J. Mol. Neurosci. *35*, 3–12.

Werner, T., Hammer, A., Wahlbuhl, M., Bösl, M.R., and Wegner, M. (2007). Multiple conserved regulatory elements with overlapping functions determine Sox10 expression in mouse embryogenesis. Nucleic Acids Res. *35*, 6526–6538.

Yang, X.J., and Seto, E. (2008). The Rpd3/Hda1 family of lysine deacetylases: from bacteria and yeast to mice and men. Nat. Rev. Mol. Cell Biol. *9*, 206–218.

Ye, F., Chen, Y., Hoang, T., Montgomery, R.L., Zhao, X.H., Bu, H., Hu, T., Taketo, M.M., van Es, J.H., Clevers, H., et al. (2009). HDAC1 and HDAC2 regulate oligodendrocyte differentiation by disrupting the beta-catenin-TCF interaction. Nat. Neurosci. *12*, 829–838.

Yu, Y., Chen, Y., Kim, B., Wang, H., Zhao, C., He, X., Liu, L., Liu, W., Wu, L.M., Mao, M., et al. (2013). Olig2 targets chromatin remodelers to enhancers to initiate oligodendrocyte differentiation. Cell *152*, 248–261.

Stem Cell Reports, Volume *3*

Supplemental Information

Neural Stem Cell Differentiation Is Dictated by Distinct Actions of Nuclear Receptor Corepressors and Histone Deacetylases

Gonçalo Castelo-Branco, Tobias Lilja, Karolina Wallenborg, Ana M. Falcao, Sueli C. Marques, Aileen Gracias, Derek Solum, Ricardo Paap, Julian Walfridsson, Ana I. Teixeira, Michael G. Rosenfeld, Kristen Jepsen, and Ola Hermanson

SUPPLEMENTARY METHODS

OPC cultures. Oli-neu cells were plated in flasks coated with 0,01% poly-L-lysine (Sigma-Aldrich) and expanded in Sato media (with 340ng/ml T3 and 400 ng/ml L-thyroxine, Sigma-Aldrich) supplemented with 1% horse serum (Invitrogen). Cells were passaged with trypsin (Invitrogen) and DNase I (Roche), and differentiated in the presence of 1mM dibutyril cAMP (Sigma-Aldrich). For lipofection or differentiation assays, Oli-neu cells were plated at the following densities: $114x10^3$ cells in 35 mm plates (Corning) or $300x10^3$ cells in 60 mm plates (Corning). For ChIP analysis, cells were expanded in 10c The postnatal OPC cells were plated in flasks coated with poly-L-ornithine and fibronectin (Sigma-Aldrich) and expanded in N1 media supplemented with FGF-2 (10ng/ml) and PDGF-BB (10ng/ml, both from R&D Systems). Cells were passaged with trypsin (Invitrogen) and DNase I (Roche), and differentiated by removal of the mitogens. For lipofection or differentiation assays, Oli-neu cells were plated at $200x10^3$ cells in 35 mm plates (Corning). For ChIP analysis, cells were expanded in 10cm plates (Corning) and allowed to grow until confluency, before collection.m plates (Corning) and allowed to grow until confluency, before collection.

Primer design. Genbank cDNA sequences or conserved regulatory sequences identified in ECR browser (Loots and Ovcharenko, 2004) were used to design gene specific primers in Primer Express 2.0 (PE Applied Biosystems) or in the Universal ProbeLibrary Assay Design Center (Roche Applied Science). The specificity of PCR primers was determined by BLAST run of the primer sequences. All primers were purchased from MWG Biotech. Primer sequences can be provided upon request.

Immunoblotting. Cells were rinsed twice with cold PBS protease inhibitor (Complete, Roche), collected by scraping and pelleted at 1000 rpm for 2 minutes at 4°C. The cells were then resuspended in NETN buffer (20mM HEPES, 150mM NaCl, 1mM EDTA and 0,5% NP40) with protease inhibitor (Complete, Roche), homogenized by passing through a 21G needle and centrifuged at 13 000 rpms for 15 minutes at 4°C. Supernatant was collected and protein concentration measured. 40µg of protein was mixed with loading buffer containing SDS, glycerol, beta-mercaptoethanol and DTT and run in 12% ReadyGel Tris-HCl (Biorad). After electrophoresis and western blot, cells were probed with the following antibodies: α-HDAC2 (2540), α-HDAC3 (2632), from Santa Cruz Biotechnology, α-Sox10 (AF2864, R&D Systems). After incubation with anti-rabbit and anti-goat HPR antibodies (Chemicon, 1:2000-1:5000), blots were developed using RPN2106 ECL Western Blotting detection reagents, from GE Healthcare.

Reverse Transcription. Total RNA was isolated from NSCs, Oli-neu and CG4 cells using RNeasy extraction kit (Qiagen), with DNAse treatment in-column. 200ng of total RNA were used with the High-Capacity cDNA Reverse Transcription Kit (Applied Biosystems), according to the manufacture's instructions and with each sample being equally divided in two tubes, a cDNA reaction tube and a negative control tube (RT-). Alternatively, Superscript II reverse transcriptase (Invitrogen) was used. Before q-PCR analysis, both cDNA and RT- were then diluted 25 or 50 times, in DNAse and RNAse free dH2O (Invitrogen).

qPCR. qRT-PCR reactions were performed in duplicates for each sample. Each PCR reaction had a final volume of 25 µl and 5µl of 25x- or 50x- diluted cDNA. RT- was run for a few samples in each run to discard genomic DNA amplification. Platinum Quantitative PCR SuperMix-UDG (Invitrogen) was used, according to the manufacture's instructions (but with a 4X dilution from the original mastermix, instead of 2X). The following thermo cycling program was used: 50°C for 2 minutes, 94°C for 2 minutes and then 40 cycles of 94° C for 30 s, 59/60ºC for 30s and 72° C for 30s on the ABI PRISM 7000 Detection System (PE Applied Biosystems, Foster City, CA, USA). A melting curve was obtained for each PCR product after each run, in order to confirm that the SYBR Green signal corresponded to a unique and specific amplicon. Random PCR products were also run in a 2-3% agarose gel to verify the size of the amplicon. Standard curves were generated for every real time PCR run and were obtained by using serial 3-fold dilutions of a sample containing the sequence of interest. Their plots were used to convert Cts (number of PCR cycles needed for a given template to be amplified to an established fluorescence threshold) into arbitrary quantities of initial template for a given sample. The expression levels were then obtained by dividing the quantity by the value of the housekeeping gene, Tata binding protein (TBP). In a few instances, hypoxanthine guanine phosphoribosyl transferase (HPRT) was used as housekeeping gene. For each individual experiment, sample values were normalized by the average sample value of the experiment. TBP assays were run at the beginning and in the middle of assays, to verify the integrity of the samples, and every time the samples were freezed/thawed. Alternatively, the delta-delta Ct method was used.

Immunocytochemistry and cell quantification. Cells were fixed in 10% formalin for 10 minutes and washed in PBS with 0.1% Triton X100, 3 times for 5 minutes. After an overnight incubation at 4ºC with the primary antibody (rat anti-myelin basic protein monoclonal (MAB386, Chemicon, 1:250), mouse RIP (Developmental Studies Hybridoma Bank, 1:100) in PBS with 1-3% bovine serum albumin (BSA), 0.1% Triton X100 and 0,02% sodium azide, the cells were washed six times for 5 minutes with PBS with 0.1% Triton X100. They were then incubated for 2 hours with an appropriate secondary antibody (donkey or goat anti-mouse and anti-rat conjugated to Alexa 488 and Alexa 546/594, 1:500, Molecular Probes/Invitrogen) in PBS with 1% bovine serum albumin (BSA) and 0.1% Triton X100. After 3 washes for 5 minutes with PBS, the cells were either counterstained with 4',6-diamidino-2-phenylindole (DAPI, Vector Laboratories). Images were acquired with a Zeiss Axiokop 2 microscope (objectives: 5x/0,25, Zeiss Fluar ∞/0,17, 10x/0,3, Zeiss NeoFluar ∞/0,17 and 20x/0,50, Zeiss Neo-Fluar ∞/0,17) and collected with a Zeiss AxioCam camera MRm (with Axiovison Rel 4.6 software). Images were processed with Adobe Photoshop CS2 version 9.0.2 and panels were assembled with Adobe Illustrator CS2 11.0.1. Quantitative immunocytochemical data of NSCs cultures represents means ± s.e.m., obtained from 3 non-overlapping 10x fields in each condition, from 3 separate independent experiments, after normalization with the number of DAPI positive cells present in the same fields. For DAPI quantification, a macro was programmed in Image J, with the following tools: "Find Edges", "Threshold", and "Analyze Particles". Cells present in clusters were counted manually with the Cell Counter Plug-in. Similar procedures were used in Fig. 4b, in which for each individual experiment, sample values were normalized by the average sample value of the experiment. Oligodendrocyte radius was measured with the AxioVision

Rel 4.6 software. MBP+ cells from 3 non-overlapping 10x field images were counted, in 4 independent experiments. For oli-neu cells, the total number of MBP+ cells with elaborate processes (>3) were counted in the entire 35mm plate in each independent experiment and then normalized by the number of DAPI+ cells in 5 random fields. For each individual experiment, sample values were normalized by the average sample value of the experiment.

RNA profiling. RNA was prepared from cultured cells of E12.5 cortex from wild-type NSCs 3 h after plating. RNA quality was assessed using the Agilent Bioanalyser 6000 Pico LabChip. 100 ng of total RNA was labelled with Cy-3 or Cy-5 using the Agilent Low RNA Input Fluorescent Linear Amplification Kit. A dye-swap design was employed. Labeled cDNA was hybridized to the Agilent 44K Whole Mouse Genome Array. Data was collected using the Agilent Microarray Scanner and Feature Extraction Software, using a Lowess option with spatial detrend to extract genes of interest with more confidence than through the use of fold-change only. Experiments were performed in triplicate, with litter-matched wild-type and mutant samples.

ChIP-seq in cortically-derived embryonic NSCs. Chromatin immunoprecipitation (ChIP) was performed following the High Cell ChIP kit # protocol from Diagenode. Five micrograms of anti-HDAC antibodies were used in each IP. Initial ChIP analysis was done with qPCR using Invitrogen Platinum SYBR Green qPCR Supermix-UDG together with site-specific primers. Chromatin immunoprecipitation followed by next generation sequencing (ChIP-Seq) was performed essentially as described before (Füllgrabe et al, 2013; Heldring et al., 2014). For ChIP-seq analysis, 5 mg of

chromatin was used in 2 separate IP's and combined into one elution. Subsequently, the DNA sequencing library was made using a kit from Illumina, except Illumina TruSeq adaptors were used to enable multiplexing. The library was analyzed by Solexa/Illumina Hi-seq. After prefiltering the raw data by removing sequenced adapters and low-quality reads, the sequence tags were aligned to the human genome (assembly hg19) with a Bowtie alignment tool (Langmead et al., 2009). To avoid any PCR-generated spikes, we allowed only one read per chromosomal position and thus eliminated PCR bias. From the filtered raw data, 2 million unique reads per sample were used for peak detection. Peak detection was per- formed using the CisGenome program (Ji et al., 2008) with a 2-sample analysis where sequenced input (1%) was used as a negative control. Peaks were called with a window statistic cutoff of 3 and a log2 fold change of 2.

REFERENCES

Füllgrabe, J., Lynch-Day, M.A., Heldring, N., Li, W., Struijk, R.B., Ma, Q., Hermanson, O., Rosenfeld, M.G., Klionsky, D.J., and Joseph, B. (2013). The histone H4 lysine 16 acetyltransferase hMOF regulates the outcome of autophagy. Nature *500*, 468-471.

Heldring, N., Nyman, U., Lönnerberg, P., Önnestam, S., Herland, A., Holmberg, J., and Hermanson, O. (2014). NCoR controls glioblastoma tumor cell characteristics. Neuro-Oncol. *16*, 241-249.

Ji, H., Jiang, H., Ma, W., Johnson, D.S., Myers, R.M., and Wong, W.H. (2008) An integrated software system for analyzing ChIP-chip and ChIP-seq data. Nat. Biotechnol. *26*, 1293–1300.

Langmead, B., Trapnell, C., Pop, M., and Salzberg, S.L. (2009) Ultrafast and

memory-efficient alignment of short DNA sequences to the human genome. Genome Biol. *10*, R25.

Loots, G.G., and Ovcharenko, I. (2004). rVISTA 2.0: evolutionary analysis of transcription factor binding sites. Nucleic Acids Res. *32*, W217-221.

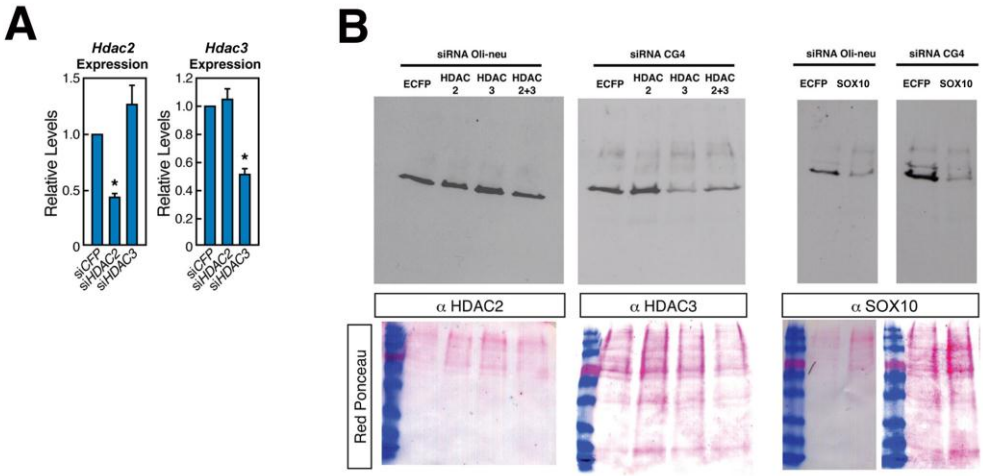

Supplementary Figure S1

A. Bars representing the levels of *Hdac2* (left panel) and *Hdac3* (right panel) mRNA as assessed by qRT-PCR after siRNA against *Hdac2* (siHDAC2) and *Hdac3* (siHDAC3).
B. Lipofection of *Hdac2* , *Hdac3* and *Sox10* siRNAs in Oli-neu and CG4 cells led to a specific decrease in the levels of the respective proteins,1 DIV after lipofection, as assessed by immunoblot with antibodies against HDAC2, HDAC3 and SOX10. Equal amounts of protein were loaded.
A-B: n=3-5 independent experiments. Error bars = S.E.M..

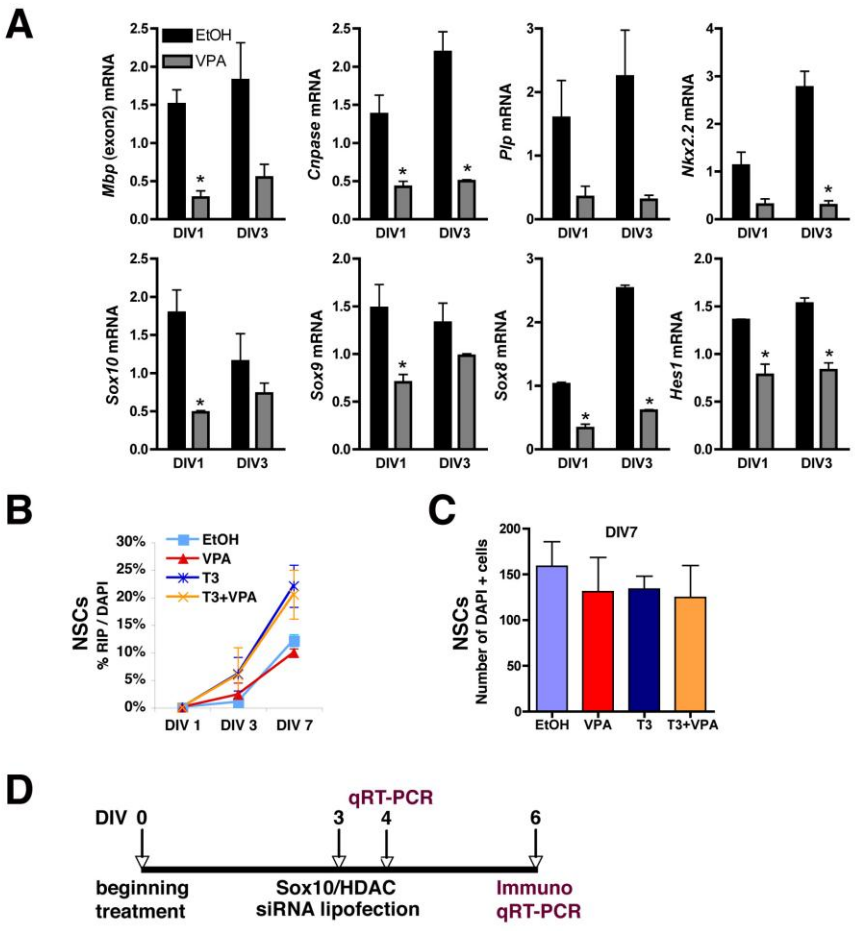

Supplementary Figure S2

A. qRT-PCR analysis of oligodendrocyte-associated transcripts revealed that HDAC inhibitor VPA in neural stem cell cultures treated with bFGF, PDGF, and IGF-2 (OLPm) led to decreased transcription of *MBP*, *CNPase*, *Nkx2.2*, *Sox10*, *Sox9*, *Sox8*, and *Hes1*.n=3-5 independent experiments.
*p<0.05 (t-test), error bars - standard error of the mean (s.e.m.).
B. The percentage of immature oligodendrocytes (RIP+) out of the total cell population (DAPI+) increased upon treatment with T3, but was not altered by VPA, as assessed by immunocytochemistry.
C. The total number of cells was not significantly affected by any of the treatments, as assessed by quantification of the number of DAPI+ cells. (B-C, n=3 independent experiments.)
D. Scheme of *Sox10/Hdac2/3* knockdown in differentiating NSCs. NSCs were differentiated for 3 DIV in absence of FGF-2 and in the presence of the different compounds. At DIV3, NSCs were lipofected with *Sox10*/*Hdac2*/*Hdac3* siRNA. Immunocytochemistry and qRT-PCR were performed with samples collected at DIV4 (1 DIV after lipofection = 1 DAT) and DIV 6 (3 DIV after lipofection = 3 DAT).

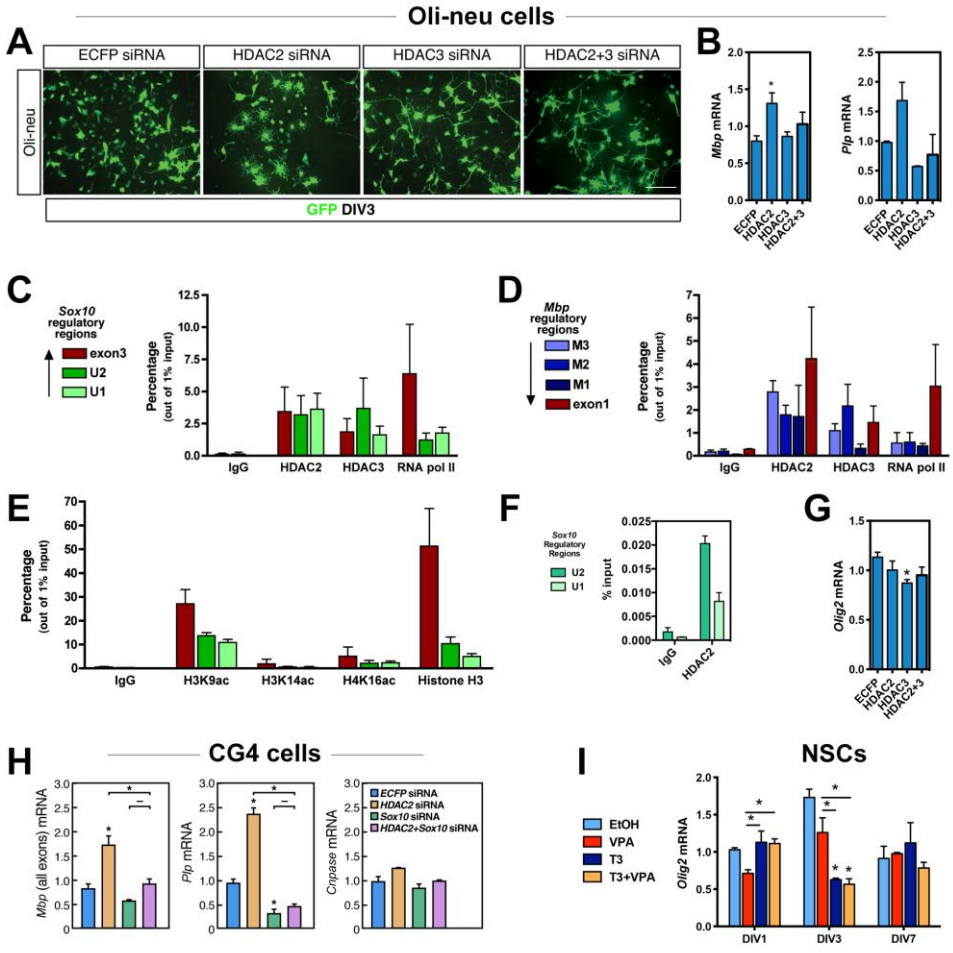

Supplementary Figure S3

A. Proliferating prenatal oligodendrocyte progenitors (Oli-neu cells) were co-lipofected with HDAC2 and/or HDAC3 siRNAs and a plasmid containing green fluorescent protein (GFP). Both siRNAs induced clear morphological changes with HDAC2 siRNA resulting in multiple short processes and HDAC3 siRNA rather to the appearance of thin, long processes. Scale bar: 60µm.
B. RT-qPCR results demonstrating *Mbp* and *Plp* mRNA levels in differentiating Oli-neu cells that were lipofected with control, HDAC2 and/or HDAC3 siRNA.
C, D, E, F. Chromatin from proliferating Oli-neu cells was cross-linked with 1% formaldehyde for 10 minutes as described in Experimental Procedures, and ChIPs were performed using antibodies against HDAC2, HDAC3, PolII, Histone H3 and the acetylated lysines H3K9, H3K14 and H4K16, followed by qPCR of regions on defined regions on the *Mbp* and *Sox10* loci.
G. RT-qPCR results demonstrating *Olig2* mRNA levels in proliferating Oli-neu cells that were lipofected with control, HDAC2 and/or HDAC3 siRNA. No increase in expression was observed.
H. RT-qPCR results demonstrating *Mbp*, *Plp*, and *Cnpase* mRNA levels in postnatal oligodendrocyte precursor (CG4) cells that were lipofected with control, HDAC2 and/or Sox10 siRNA.
I. RT-qPCR results demonstrating *Olig2* mRNA levels in NSCs that had been treated with vehicle, VPA and/or T3. No increase in expression was observed.
A, B, G, H, I: n=3-5 independent experiments. **C, D, E, F:** n=2-3 independent experiments. Error bars = S.E.M..

A

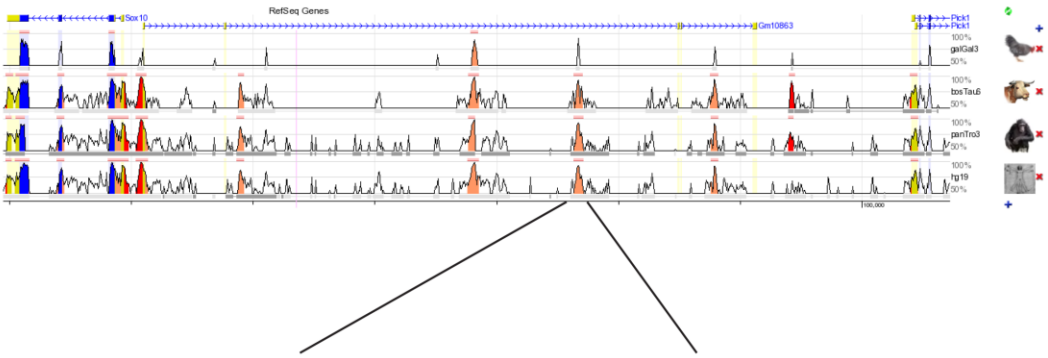

Sox10 **U2 enhancer sequence in mouse (mm10)/human (hg19)**

Conserved SOX_Q6 binding sites in blue (analysis with ECR browser and RVISTA 2.0)
ChIP-qPCR U2 amplicon in red

```
mm10    CACTTCTCTCAGCCTCAGTTTCCCTCTCTTGTAATACAGGGGTGAATTGTCTCCATAACC
hg19    CATCTCTCTGGGTCTCAGTTTCCCCCTCT-ATAACACCAGGG--GCTGGTCTTCATGATC

mm10    GCAAGACCCTCTCCAGCTGTGCCCTCCTGTGACTGAGAG--TCTGAGAGCAGAGGCAGGA
hg19    CCAGGGCCCTCCCCAGCTGTGCCCATCTGCAACTGTGAGATTCTGAGAGCAGAGGAGGGA

mm10    AGGCAAGATGGGGCCCCTCTTTCCCCACCTCCTCTCCCTGTCCCCCAGGGTCACCCCAAA
hg19    AGGCGGGATGG--CCCCTCTTTCCCCACCGCCTCTCTCTGTCCCCCAGGGTCACCCCAAA

mm10    GCCGCCCCT--CCCCAGCTCCCTGGGACTTCCCTGCAGCTGCAGAC-TGGGGAGACAATC
hg19    GCCGCCCCCTCCCCCGGCTCCCTGGAACTTCCCTGCAGCTGCAGGCCTGGTGAGACAATT

mm10    GGGTGCTTTAGAGAAATACATTTTGGGCTAATTTGCCATGCAGAAGTGTTTCTCTTACC
hg19    GGGTGTTTTAGAGAAATACATTTTTGGGCTAATTTGCCATGCATAAGTGTTTCTCTTACC

mm10    CTTTAAAGGCAGAGAACAAAGAGACCTTTCTGTGCCTGGGCAGGCTGCTGGGAAGGGGAC
hg19    CTTTAAAGGCGGAGAACAAAGAGGTCTTTCTGTGCCCAGGCAGGCTGCTGGGGAGGGGA-

mm10    CGCAGCTGTA-GGGGCTGTCGAC---CCTCCCTCCCTCCATCCCAGTGAGCATCCCAGCA
hg19    CGCAGCTGTACTGGGCTGGCGACCCTCCTCCCTCCCCCCATCCCTGCGAGCGCCCCACCA

mm10    CACAGCCCCCGTGTCCCACCCCCGCCCCCAAGAGGGACAGCCTGGACTTTCCCAGCCTC
hg19    CACCG---------CCCACCGC---CCCCCAGAAGAGACAGCCCGGACTTTCCCAGCCTC

mm10    CCCCAGTTGCCCAGCCGGG----------------------------------CCCAGCCCC
hg19    CCCCAGTCTCCTACCCCGGCTGCCTCTGAGGCTCCTCTGGCCCTGCCTTGCCCCAGCTCC

mm10    CTCCCACCAGCTGCCCCAGGCGAGAGGGAAAGTGTGCGTGGGT-GGCGACTGGGTGGGGA
hg19    CCCTC-CCAGCTGCCCCAGGCAAGAGGGAAAGTGTGTGTGGGTGGGTGGATGGACGGGGA

mm10    GGGGC--ACCAGGAGAGAAAGCCATTCTCCACGTGGTTGTGGTG
hg19    GGGGCGTGCATGGAGAGACAGCGGCTTTCCATGTGGCCCGGGTG
```

B

Enriched binding motif for SOX2
(source JASPAR database, ID MA0143.1,
derived from Chen et al., Cell 2008)

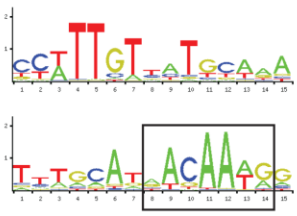

Reverse complement

Supplementary Figure S4

A. A conserved SOX2 binding site (blue) in the U2 enhancer (red) of the *Sox10* gene found in mouse and human.

B. A similar site detected by ChiP-Seq in embryonic stem (ES) cells.

Reference:
Chen et al. (2008) "Integration of external signaling pathways with the core transcriptional network in embryonic stem cells. Cell *133*, 1106-17.

CASTELO-BRANCO et al, SUPPLEMENTARY TABLE 1.
Gene expression data underlying heatmap in Figure 2B.

PEAK FOLD	ACC #	DESCRIPTION
25.14	M37335	proteolipid protein (myelin)
28.74	M11533	myelin basic protein
7.47	M63801	gap junction membrane channel protein alpha 1
4.84	X16202	
4.59	V00746	histocompability 2, K region
4.41	M69069	histocompability 2, D region locus 1
4.19	AI117211	histocompability 2, L region
3.79	C78850	RIKEN cDNA 1300007C21 gene
3.79	L26836	ATP-binding cassette, sub-family D (ALD), member 3
4.18	L47480	bone morphogenetic protein 4
5.14	M28730	tubulin, beta 4
4.00	M16472	proteolipid protein (myelin)
4.04	AF031127	
3.75	K02236	metallothionein 2
3.39	U31566	NK2 transcription factor related, locus 2 (Drosophila)
3.12	AJ223206	scrapie responsive gene 1
3.16	M26071	coagulation factor III
3.52	X52490	histocompability 2, D region
2.79	M25944	carbonic anhydrase 2
2.78	X01838	beta-2 microglobulin
2.77	X00246	histocompability 2, D region locus 1
2.72	AJ006474	carbonic anhydrase 3
2.95	AI847230	
2.97	AI851348	
2.73	U73521	solute carrier family 1, member 1
2.60	AI840267	sirtuin 2 (silent mating type information regulation 2, homolog) 2 (S. cerevisiae)
2.69	J04627	methylenetetrahydrofolate dehydrogenase (NAD+ dependent)
2.35	M21265	stearoyl-Coenzyme A desaturase 1
2.24	J02652	malic enzyme, supernatant
2.42	L06115	CD9 antigen
2.58	M18837	
2.43	M58156	MHC (A.CA/J(H-2K-f) class I antigen
2.44	AI850558	
2.17	M27134	histocompability 2, K region locus 2
2.98	AW060549	RIKEN cDNA 13000007C21 gene
2.67	AF017994	mesoderm specific transcript
2.56	M17327	
2.69	AI845796	RIKEN cDNA 231000B05 gene
2.22	AI842277	insulin-like growth factor binding 3.
5.20	U19582	claudin 11
3.70	M63801	gap junction membran channel protein alpha 1
3.57	L22144	S100 protein, beta polypeptide, neural
3.44	AB017270	transmembrane protein with EGF-like and two follistatin-like domains 2
3.45	AW046181	serum/glucocorticoid regulated kinase
3.31	U51000	distal-less homeobox 1
3.05	AI845514	ATP-binding cassette, sub-family A (ABC1), member 1
2.66	AW125478	protease, serine, 11 (igf binding)
2.67	AI840191	expressed sequence AW547365
2.28	D83277	RAB33A, member of RAS oncogene family

2.23	AI001972	inhibitor of DNA binding 4
2.21	AW124983	epidermal growth factor receptor pathway substrate 15
2.19	L12447	insulin-like growth factor binding protein 5
2.20	AB017026	cDNA sequence AB017026
2.18	AI842472	
2.23	AI848201	RIKEN cDNA 1700006H23 gene
2.33	AF031127	
2.17	AW124196	RIKEN cDNA 5530600A 18 gene
2.21	X66449	S100 calcium binding protein A6 (calcyclin)
2.24	AI847795	
2.24	U86090	kinesin family member 5B
2.39	U39738	p21 (CDKN1A)-activated kinase 3
2.53	AW122114	RIKEN cDNA C0300448H19 gene
2.58	AW061337	adenylate kinase 4
2.27	L49507	cyclin G
2.22	AW125874	RIKEN CDNA 3010001M15 gene
2.23	AW046627	
2.16	AI842065	expressed sequence AU046135
2.23	AW125390	RIKEN cDNA 1110004C05 gene
2.26	AA016517	RIKEN cDNA 1500005102 gene
2.15	AI844626	glycine amidinotransferases (L-arginine glycine aminotransferas)
2.30	AV347220	endothelial differentiation sphingolipid G-protein-coupled receptor 1
2.35	X05862	
-2.81	AI851048	RIKEN cDNA 1810030E20 gene
-2.60	AI854154	DNA segment, Chr 9, Wayne State University 18, expressed
-2.64	AI853439	
-2.90	X61397	carbonic anhydrase-like sequence 1
-4.24	AA880275	metallothionein-I activator
-6.72	AA874329	
-3.67	L04961	inactive X specific transcripts
-7.34	AW047207	RIKEN cDNA 1810037I17 gene
-4.75	AI853444	RIKEN cDNA 2610042L04 gene
-3.77	AI853444	RIKEN cDNA 2610042L04 gene
-6.33	AI854020	cysteine dioxygenase 1, cytosolic
-4.03	AF084642	retinaldehyde binding protein 1
-2.94	AF000294	peroxisome proliferator activated receptor binding protein
-4.07	AW228316	RIKEN cDNA 2310046G15 gene
-3.23	AB028241	casein kinase 1, epsilon
-2.74	AW258842	RIKEN cDNA 2510049I19 gene
-2.27	U32329	endothelin receptor type B
-2.43	AI325791	expressed sequence AI507524
-2.36	U22399	cyclin-dependent kinase inhibitor 1C (p57)
-2.73	X15986	lectin, galactose binding, soluble 1